

RESEARCH ARTICLE

Echolocation click parameters and biosonar behaviour of the dwarf sperm whale (*Kogia sima*)

Chloe E. Malinka^{1,*}, Pernille Tønnesen¹, Charlotte A. Dunn^{2,3}, Diane E. Claridge^{2,3}, Tess Gridley^{4,5}, Simon H. Elwen^{4,5} and Peter Teglberg Madsen¹

ABSTRACT

Dwarf sperm whales (*Kogia sima*) are small toothed whales that produce narrow-band high-frequency (NBHF) echolocation clicks. Such NBHF clicks, subject to high levels of acoustic absorption, are usually produced by small, shallow-diving odontocetes, such as porpoises, in keeping with their short-range echolocation and fast click rates. Here, we sought to address the problem of how the little-studied and deep-diving *Kogia* can hunt with NBHF clicks in the deep sea. Specifically, we tested the hypotheses that *Kogia* produce NBHF clicks with longer inter-click intervals (ICIs), higher directionality and higher source levels (SLs) compared with other NBHF species. We did this by deploying an autonomous deep-water vertical hydrophone array in the Bahamas, where no other NBHF species are present, and by taking opportunistic recordings of a close-range *Kogia sima* in a South African harbour. Parameters from on-axis clicks ($n=46$) in the deep revealed very narrow-band clicks (root mean squared bandwidth, BW_{RMS} , of 3 ± 1 kHz), with SLs of up to 197 dB re. 1 μ Pa peak-to-peak (μ Pa_{pp}) at 1 m, and a half-power beamwidth of 8.8 deg. Their ICIs (mode of 245 ms) were much longer than those of porpoises (<100 ms), suggesting an inspection range that is longer than detection ranges of single prey, perhaps to facilitate auditory streaming of a complex echo scene. On-axis clicks in the shallow harbour ($n=870$) had ICIs and SLs in keeping with source parameters of other NBHF cetaceans. Thus, in the deep, dwarf sperm whales use a directional, but short-range echolocation system with moderate SLs, suggesting a reliable mesopelagic prey habitat.

KEY WORDS: Beam pattern, Bioacoustics, Hydrophone array, Narrow-band high-frequency, Passive acoustic monitoring, Source parameters

INTRODUCTION


Echolocating toothed whales navigate and detect prey by emitting powerful clicks and subsequently processing the returning echoes to form an actively generated auditory scene. This active sensory modality has allowed toothed whales to specialize in a range of aquatic food niches from mesopelagic depths to shallow rivers and

estuaries (Madsen and Surlykke, 2013). The deep-diving sperm whales, pilot whales, belugas, narwhals and beaked whales are among the largest predators on the planet, and have evolved low (<30 kHz) to medium (~30–80 kHz) frequency, high-power biosonar systems sampling at low rates to find and target mainly cephalopod prey at mesopelagic and bathypelagic depths (Au et al., 1987; Møhl et al., 2003; Johnson et al., 2004, 2006; Aguilar de Soto et al., 2008; Koblitiz et al., 2016; Pedersen et al., in review). Conversely, some of the smallest toothed whales, including river dolphins (e.g. *Inia*), small dolphins (e.g. *Cephalorhynchus*, *Lagenorhynchus/Sagmatius*) and porpoises (e.g. *Phocoena*, *Phocoenoides*), employ high-frequency, low-power biosonars, sampling at fast rates in keeping with finding small prey at short ranges in their often shallow, acoustically cluttered habitats (Jensen et al., 2013; Kyhn et al., 2009, 2010, 2013; Ladegaard et al., 2015). High-frequency signals are more suited to detecting/discriminating small prey items (Au, 1993), and may facilitate acoustic crypsis from eavesdropping killer whales (Møhl and Andersen, 1973). Thus, mounting evidence suggests that spectral emphasis, output levels and biosonar sampling rates have broadly co-evolved with foraging niche adaptations, predation pressure, body size and diving capabilities in toothed whales, similar to the sensory niche adaptation observed in the biosonar guilds of bats (Schnitzler and Kalko, 2001).

It has recently been argued that such inverse scaling of the spectral emphasis of clicks with body size serves to maintain a stable acoustic field of view of around 10 deg in echolocating toothed whales (Jensen et al., 2018). The narrowness of the acoustic field of view exists in a trade-off between high source levels (SLs) and clutter rejection on the one hand, and beamwidths wide enough to make prey search efficient on the other. Large toothed whales radiate lower-frequency clicks from their large melons and small toothed whales radiate high-frequency clicks from their small melons, resulting in broadly similar ratios between dominant wavelengths and radiating apertures across three orders of magnitude in body mass. Harbour porpoises (*Phocoena phocoena*), for example, are known to generally occupy coastal habitats and produce narrow-band high-frequency (NBHF) clicks centred on ~125 kHz at low SLs [150–190 dB re. 1 μ Pa peak-to-peak (μ Pa_{pp}) at 1 m] and short inter-click intervals (ICIs) below 100 ms. Such click properties are shared among the other porpoise species and have evolved convergently in dolphins in the *Cephalorhynchus* genus that are also often hunting in coastal habitats (Kyhn et al., 2009, 2010), leading to the proposition that NBHF clicks evolved to facilitate echolocation in cluttered habitats for small toothed whales (Ketten, 2000). Conversely, the deep-diving sperm whale (*Physeter macrocephalus*), which can reach a length of up to 18 m, employs a long-range echolocation system (of the order of hundreds of metres) via clicks with very high source levels (up to 240 dB re. 1 μ Pa_{pp}

¹Zoophysiology, Department of Biology, Aarhus University, 8000 Aarhus, Denmark. ²Bahamas Marine Mammal Research Organisation (BMMRO), Sandy Point, Abaco, Bahamas. ³Sea Mammal Research Unit, University of St Andrews, St Andrews KY16 8LB, UK. ⁴Department of Botany and Zoology, Stellenbosch University, Stellenbosch 7605, South Africa. ⁵Sea Search Research and Conservation, Muizenberg, Cape Town 7945, South Africa.

*Author for correspondence (chloe.e.malinka@bio.au.dk)

 C.E.M., 0000-0003-0138-8388; P.T., 0000-0002-0869-6490; C.A.D., 0000-0002-4274-7239; D.E.C., 0000-0002-9028-8647; T.G., 0000-0003-0925-5782; S.H.E., 0000-0002-7467-6121; P.T.M., 0000-0002-5208-5259

List of abbreviations

ASL	apparent source level
BW	bandwidth
DI	directivity index
DT	detection threshold
EFD	energy flux density
EPR	equivalent piston radius
F_c	centroid frequency
F_p	peak frequency
ICI	inter-click interval
NBHF	narrow-band high-frequency
PAM	passive acoustic monitoring
pp	peak-to-peak
Q	resonant quality factor
RHIB	rigid hull inflatable boat
RL	received level
RMS	root mean square
SL	source level
TL	transmission loss
TOL	third octave level
TS	target strength

at 1 m), high directionality (directionality index of >27 dB), low absorption with peak frequencies at 15–20 kHz, and ICIs between 0.4 and 1 s (Møhl et al., 2000, 2003; Madsen et al., 2002, 2007; Tønnesen et al., 2020).

However, not all toothed whales conform to that scaling; a close relative of the sperm whale, the much smaller *Kogia*, the genus of both the dwarf [*Kogia sima* (Owen 1866)] and pygmy sperm whales [*Kogia breviceps* (Blainville 1838)], also produce NBHF clicks despite their presumed deep-sea foraging. Their deep-diving behaviour has been inferred from visual observations over continental slopes and shelf breaks (Caldwell and Caldwell, 1989; Baumgartner et al., 2001; MacLeod et al., 2004; Dunphy-Daly et al., 2008), and from deep-sea squid beaks and meso-benthopelagic fish otoliths in the stomach contents of stranded *Kogia* (Plön, 2004; Elwen et al., 2013; Staudinger et al., 2014). It is therefore puzzling and counterintuitive that *Kogia*, in evolutionary convergence with porpoises, also produce NBHF echolocation clicks (Madsen et al., 2005a), as this click type suffers from an absorption that is ~40 times greater than that of clicks made by sperm whales foraging in the same environment. In the very different habitats of *Kogia*, porpoises and *Cephalorhynchus* dolphins, echolocators would be faced with different challenges in terms of prey ranges, reverberation, clutter and noise, yet *Kogia* have, in convergence with the shallow-diving species, evolved to produce NBHF biosonar clicks. Some acoustic parameters of *Kogia* clicks (e.g. peak frequency, bandwidth, duration, etc.) have been reported from stranded *Kogia* held in captivity for rehabilitation (Thomas et al., 1990; Ridgway and Carder, 2001; Marten, 2000; Madsen et al., 2005a) and from recent single-channel field recordings (Merkens et al., 2018; Merkens and Oleson, 2018; Hodge et al., 2018; Hildebrand et al., 2019; Griffiths et al., 2020). Here, we sought to obtain a deeper quantitative understanding of how *Kogia* can echolocate to find deep-sea prey using clicks with spectral properties suited for short-range echolocation.

The much larger body (4–6 times heavier) of *Kogia* compared with that of other NBHF odontocetes means that the aperture of its sound-producing head is expected to be 2–3 times larger with respect to the dominant wavelengths of a NBHF click. This suggests that their acoustic field of view should be narrower by the same factor on a linear scale, and the corresponding directivity index (DI)

should be 6–9 dB higher than in other NBHF species (Au, 1993). From their deep-water prey, it is predicted that *Kogia* would search for prey over longer ranges (hundreds of metres) than shallow-diving NBHF species (tens of metres), making high directionality favourable. Such predictions prompt the hypotheses that they use higher SLs and longer ICIs to facilitate longer range echolocation. In this study, we tested these hypotheses by quantifying the biosonar source parameters and acoustic behaviour of wild *Kogia*. Specifically, we measured the SL, directionality and beam pattern of *Kogia* clicks, uniquely made possible via recordings made with a novel deep-water vertical hydrophone array deployed with concurrent visual sightings of *Kogia sima*. These data are presented in conjunction with visually validated and close-range, shallow-water, single-channel recordings of the same species.

MATERIALS AND METHODS

Clicks of *Kogia* were recorded in two locations with two methods: (1) using deep-water vertical arrays off the continental shelf edge in the Bahamas, and (2) opportunistically using a single-channel recorder in Cape Town harbour, South Africa.

Recording and calibration

Array recordings were made using two custom-built vertical hydrophone arrays, each composed of seven autonomously recording and sample-synchronized SoundTraps (ST300-HF, Ocean Instruments, Auckland, New Zealand; <http://www.oceaninstruments.co.nz/>) (see Malinka et al., 2020). The SoundTraps were spaced ~14 m apart (13.82–14.21 m), as informed by simulations of predicted *Kogia* beam patterns, for an overall aperture of 84 m. Animals can theoretically be localized (with less than 30% range error) out to ~840 m around the array (10× the array aperture), based on increasing deterioration in localization accuracy with increasing range (e.g. Kyhn et al., 2009; Macaulay et al., 2017; Malinka et al., 2020).

Prior to data collection, artificial porpoise-like clicks were projected at a SoundTrap attached to the array cable to quantify the degree of shading behind the cable, resulting in a maximal nominal loss of 1.5 dB. All SoundTraps on the arrays were calibrated against a Reson 4034 hydrophone (Teledyne Marine, Slangerup, Denmark) in a 3 m deep cedar tank (in 10 kHz steps up to 200 kHz). Each device sampled at 576 kHz with 16-bit resolution with a high gain setting (resulting in clip levels ranging from 174 to 180 dB re. 1 μ Pa at 130 kHz). The single SoundTrap used in South Africa was not available for calibration, and so an average from 19 other calibrated SoundTraps was applied to this recorder, for an estimated clip level of 174 dB re. 1 μ Pa at 130 kHz. All calibrated devices showed system clip levels varying ± 2 dB, from 10 kHz to 90 kHz, and by ± 1 dB in the 100–190 kHz range relevant to this study.

Two temperature and inclinometer sensors (Star Oddi DST tilt-and-depth sensors; www.star-oddi.com), attached to the body of the peripheral SoundTraps, confirmed that the arrays were straight throughout deployments with *Kogia* clicks. Deviations from hanging perfectly vertically (0 deg) were included in calculating error ($\sin\theta \times \text{range}$) in the depth of the localizations. Temperature informed the sound speed used in transmission calculations.

Data collection**Shelf edge, Bahamas**

Array data were collected in May–June 2018, in the NE Providence Channel, south of Great Abaco Island, in the Bahamas (~25°54.0'N, ~77°20.0'W) during daylight hours. This field site was chosen because *Kogia* are commonly observed there (MacLeod et al., 2004;

Claridge, 2006; Dunphy-Daly et al., 2008; Dunn and Claridge, 2014), and within 4 km from shore, the seafloor steeply drops to depths >3000 m, enabling daily fieldwork access with a small boat. Importantly, beyond the two species of *Kogia*, no other NBHF pulse-producing species are known to occur in Bahamian waters.

The vertical passive acoustic array was deployed from a rigid hull inflatable boat (RHIB) on 18 occasions. The array was suspended below a top float, with an optional rope (single cross-braid polyester) extension (of 100 or 200 m) between the top float and the array, making the depths of top and bottom hydrophones 11 m and 95 m, 111 m and 195 m, or 211 m and 295 m (for 16%, 15% and 69% of the total recording time, respectively). Both the top float and a rod of trawl buoys positioned between the extension rope and the array contained radio transmitters (MM150, Advanced Telemetry Systems) to facilitate recovery (for details, see Malinka et al., 2020). A ~10 kg terminal weight was added to the bottom of the array to keep it vertical and linear in the water. One array was deployed at the start of a day in the absence of any visual or acoustic cues, and a combination of visual and acoustic observation was used to prompt the deployment of the second array. Acoustic observation entailed suspending a Reson TC4013 hydrophone a few metres below the RHIB, connected to a custom-built pre-filter (high pass 40 kHz) and click-detector box, connected to headphones. If clicks were heard on the headphones, the second array was deployed. Looking and listening stations were informed by past visual observations of *Kogia* presented in Dunphy-Daly et al. (2008).

A total of ~20 min of *Kogia* echolocation clicks were recorded in the deep and natural habitat by the array over 74.6 h of effort. These were obtained in two ~10 min continuous sections ('period A' and 'period B'), recorded on two consecutive days (10 and 11 May 2018), both when the array was at a maximum depth of ~95 m. Period A coincided with visual observation of a pair of *Kogia sima* and no other odontocetes, with species identification visually confirmed by experienced local researchers. Period B had no visual detections of any odontocete. During other deployments, the only

other odontocete species visually observed were Blainville's beaked whale (*Mesoplodon densirostris*) producing frequency-modulated clicks around 40 kHz (Madsen et al., 2013). For both periods A and B, the array was slightly tilted at 9 deg off vertical, but in both instances, the tilt measurement at the top and bottom of the array was <1 deg apart, indicating straightness, but translating to errors in the calculated depths of localizations of 4% or 15% for the localization ranges in periods A and B, respectively (Table 1). Within these two periods, a total of 8636 clicks were detected and classified as *Kogia* across all channels. As many of these click recordings represented the same click, a subset of 1492 clicks were available for ICI measurements (noting that each click was not necessarily detected on all channels). From these detections, 46 clicks (0.5%) fulfilled the on-axis criteria (detailed below), had localizations whose errors in apparent source level (ASL) were <3 dB, and were used in source parameter measurement. A subset of 21 clicks (0.2%) had localizations whose errors in angular incidence were <3 deg and were used in beam pattern estimation.

Sound speed was estimated to be 1535 m s⁻¹ based on the mean water temperature measured by sensors attached to both peripheral SoundTraps on the array of 25.0°C (mean of 25.8°C at 11 m, and mean of 24.2°C at 95 m, for the two deployments in which *Kogia* clicks were detected), and a local salinity of 36.5 ppm (Medwin, 1975; Sato and Benoit-Bird, 2017). This constant sound speed was used in localization calculations. Accordingly, potential errors arising from surface propagation were investigated using the 'AcTUP' (Duncan and Maggi, 2006) MATLAB toolbox (2017a, Mathworks, Natick, MA, USA), which confirmed straightness of ray paths for the ranges considered here.

Cape Town harbour, South Africa

Opportunistic recordings (~4 h) of a single wild *Kogia sima* were made during daylight hours (9 and 11 November 2016) in Cape Town harbour (depth of 6–8 m), South Africa (~33°54'S, ~18°26'E), with a single high-frequency digital recorder (SoundTrap HF300,

Table 1. Source parameters for all on-axis *Kogia* echolocation clicks

Parameter	Array recording, Bahamas		Single-channel recording, Cape Town harbour, South Africa		Unit
	Mean±s.d.	Median (range) or [95% CI]	Mean±s.d.	Median (range)	
SL _{pp}	186±6	185 (174–197)	158±12	157 (125–193)	dB re. 1 µPa at 1 m
SL _{RMS}	174±6	174 (162–186)	146±12	146 (113–181)	dB re. 1 µPa at 1 m
SL _{EFD}	135±6	134 (123–147)	105±11	104 (72–137)	dB re. 1 µPa ² s at 1m
Duration (–10 dB)	142±37	142 (71–205)	77±29	68 (32–202)	µs
F _c	123±4	122 (118–129)	129±2	129 (120–142)	kHz
F _p	123±4	122 (117–130)	129±3	129 (118–140)	kHz
BW _{-3 dB}	4±2	4 (2–9)	8±3	8 (2–18)	kHz
BW _{-10 dB}	8±3	7 (5–16)	15±4	16 (6–31)	kHz
BW _{RMS}	3±1	2 (1–7)	5±2	5 (2–14)	kHz
Q _{RMS}	56±20	56 (19–94)	31±12	28 (10–82)	(unitless)
DI	27.0	[25.2–28.5]	n/a	n/a	dB
Equivalent piston radius	4.2	[3.7–5.5]	n/a	n/a	cm
Beamwidth	8.8	[7.0–10.3]	n/a	n/a	deg
ICI	209±75	228 (23–489)	51±34	43 (4–347)	ms
Range	405±189	479 (134–718)	9±7	7 (0.5–42)	m
Depth of localizations	94±113	47 (1–392)	n/a	n/a	m
Depth of recorder	11–95	n/a	~3	n/a	m
Depth of water at recording site	(A) ~400 (B) ~900	n/a	~7	6–8	m
N clicks (source parameters)	46		870		n/a
N clicks (beam pattern estimation)	21		n/a		n/a

Only those passing criteria and with reasonable localization errors are shown. Some measurements are indicated separately for the 2 array deployments with *Kogia* clicks (periods A and B; see Materials and Methods). SL, source level; pp, peak-to-peak; RMS, root mean square; EFD, energy flux density; F_c, centroid frequency; F_p, peak frequency; BW, bandwidth; Q, quality factor; DI, directivity index; ICI, inter-click interval; CI, confidence interval.

sampling at 576 kHz) suspended (depth of ~3 m) from a moored RHIB. The close range to the animal facilitated species identification, which was based on the size and shape of the dorsal fin (Fig. S1). Audio recordings were made in conjunction with time-aligned voice notes detailing the orientation and distance of the visible and close-by animal relative to the recorder, as estimated by experienced observers. The animal was mostly slowly swimming in circles at the surface, but also regularly approached and came within metres of the hydrophone. The animal was clearly observed throughout recordings and no other cetaceans were observed. The harbour was active, and boats were motoring in and out of the harbour throughout the deployment. A total of 16,805 clicks were detected and classified as *Kogia*, of which 870 (5.2%) fulfilled on-axis criteria (detailed below).

Analysis

Detection, classification and localization

The click detection module in PAMGuard (www.pamguard.org, version 2.01.03; Gillespie et al., 2008) was used to detect and extract all transient signals above a 10 dB signal-to-noise ratio (SNR) threshold above background noise on filtered data (6-pole Chebyshev band-pass filter from 90 to 180 kHz). Small, unfiltered sound clips containing the full click waveform were saved upon each detection. Clicks were classified as *Kogia* based on peak frequency and by comparing energy in different frequency bands using the inbuilt click classifier. Manual supervision was applied to validate click detection and classification, including checking amplitude modulation and excluding echoes. Clips of raw WAV files of each classified click were then used in subsequent analysis. For the array data, clicks were localized using the Larger Aperture 3D Localizer module, using a time delay-based ‘Mimplex’ algorithm described by Macaulay et al. (2017). Only clicks that were detected on multiple channels and localized were considered in further analyses.

On-axis click selection

On-axis clicks, defined as being recorded at the centre of the sound beam, were selected using established criteria (Kyhn et al., 2009, 2010, 2013; Madsen and Wahlberg, 2007; Jensen et al., 2013; Ladegaard et al., 2015). It is important to use on-axis clicks for source parameter quantification given the high directionality of toothed whale biosonars, resulting in high distortion of clicks recorded off-axis. Specifically, on-axis clicks should be: (i) detected on multiple channels and localized; and (ii) part of a series of clicks scanning across the array; whereby (iii) the highest received level (RL) occurred on any of the central five channels, for the highest likelihood of being on-axis in the vertical plane; (iv) the click had the greatest RL within a scan, for the highest likelihood of being on-axis in the horizontal plane; and (v) localizations were within $10\times$ the aperture of the array. Source parameters were extracted for clicks that met all of these criteria. Only criterion (ii) could be applied to the harbour recordings because of only using a single-channel recorder. Directionality of *Kogia* clicks is sufficiently high that even in a captive recording environment, clicks were only detected by Madsen et al. (2005a) when the animal was close to the hydrophone within the pool, or, if at a distance, was directly facing the hydrophone. This suspected high directionality of *Kogia* clicks means that of the clicks that were detected, a significant proportion are expected to be recorded on-axis.

Source parameter estimation

Pre-filtered (10 kHz high-pass 4-pole Butterworth) clips of click recordings were brought into MATLAB using the PamBinaries

library for MATLAB (<https://sourceforge.net/projects/pamguard/files/Matlab/>). Click clips were digitally high-pass filtered (80 kHz, 4-pole Butterworth). Click source parameters from on-axis clicks were extracted following Au (1993), Madsen and Wahlberg (2007), and Ladegaard et al. (2015). ASLs were back-calculated (*sensu* Møhl et al., 2000) given the localized ranges (r , in metres), RLs and estimated transmission loss (TL), assuming spherical spreading losses (of $20\log_{10}r$) (Urlick, 1983). The calculation for TL also relies on a range-dependent and frequency-specific absorption coefficient (α , in dB m^{-1}), but rather than assuming a single value of α based on, for example, the peak or centroid frequency, α was computed for each bin in the power spectrum (bin size ~1 kHz; Ainslie and McColm, 1998) prior to inverse transformation back to a waveform from which all click parameter quantifications were drawn (*sensu* Pedersen et al., 2021). This compensation is especially important for broadband clicks, but is good practice to maintain for narrow-band clicks.

ASL values calculated for each hydrophone in the array were interpolated to determine the point along the array at which the acoustic axis was pointing. Therefore, it was not assumed that the channel that recorded the on-axis click candidate with the highest ASL was collected at exactly 0 deg relative to the beam axis. Clicks were rejected if the localization error resulted in a change in ASL of >3 dB on the on-axis channel (*sensu* Kyhn et al., 2013). ASL values for the single-channel recording were calculated using the RL and the visually observed ranges to the animal; recorded distances to the animal were interpolated, and if the time after the last sighting was greater than 5 s, then the click was discarded from further analysis as no reliable range estimation could be obtained.

Click clips were interpolated (MATLAB *interp* function) by a factor of 10 to better estimate signal window length (*sensu* Ladegaard et al., 2015), and click duration was calculated as the interval between the -10 dB points relative to the peak of the interpolated click envelope (Madsen et al., 2005b). The power spectrum of each click was computed (FFT size 1024 to provide a spectral resolution of 562 Hz). Peak frequency (F_p) was calculated as the highest value in the power spectra, and centroid frequency (F_c) divided a spectrum into two halves of equal energy on a linear scale. Bandwidth (BW), frequency minimum and frequency maximum were calculated at -3 dB and -10 dB thresholds around F_p in the power spectrum (*sensu* Au, 1993). The RMS of bandwidth (BW_{RMS}) was additionally measured by taking the standard deviation around the F_c . The resonant quality factor (Q_{RMS}) was calculated by dividing F_c by the BW_{RMS} , whereby a greater Q indicates a lower rate of energy loss relative to the resonator's energy, such that the oscillations diminish more slowly (Au, 1993). RLs were quantified as peak-to-peak amplitude (pp), root mean square amplitude (RMS) and energy flux density (EFD) level, where the last two were computed over the click duration. The RL EFD level was calculated as the RMS amplitude plus $10\log_{10}(\text{click duration})$ (measured in s) (*sensu* Madsen et al., 2005b). All clicks that were classified as *Kogia* and were within a scan, whether they were considered to be collected on-axis or not, contributed to measurements of ICI.

Beam pattern estimation

To resolve the beam pattern, the angles and intensities of on-axis clicks, as recorded on an array of hydrophones, were used to fit the transmission pattern of a flat and circular piston of varying diameter of 2–15 cm (in steps of 0.1 cm) (Strother and Mogus, 1970; Au et al., 1978; Beedholm and Møhl, 2006). The piston model describes the beam attenuation relative to the angle from the acoustic

axis, relying only on the waveform of an on-axis echolocation click and the functional aperture of the sound generator. It has previously been used as a model for the radiation of toothed whale biosonar (Au, 1993; Beedholm and Møhl, 2006; Kyhn et al., 2010; Koblitz et al., 2012; Jensen et al., 2015; Finneran et al., 2016) and can successfully model at ± 30 deg around the beam axis (Macaulay et al., 2020).

For each on-axis and localized click, the location of the beam axis relative to each array channel is calculable. Therefore, the off-axis angle relative to the acoustic axis of the click, as recorded on all other hydrophones, is also calculable. The ASL of each on-axis click was normalized relative to the channel with the highest back-calculated ASL. Off-axis angles and normalized ASLs were used to resolve the biosonar transmission beam pattern (Madsen and Wahlberg, 2007). Clicks were not included in the beam pattern estimation if the localization error resulted in a change in angle of incidence of >3 deg. As we did not have a movement sensor on the animal, we could not measure the tilt of the emitter, and so rotational symmetry of the beam was assumed. The goodness of fit was calculated for each diameter and then bootstrapped for confidence intervals (*sensu* Jensen et al., 2015), including errors from cable shading. The half-power (-3 dB) beamwidth was calculated from the beam pattern and the transmission DI was fitted to this. The DI was calculated as $DI = 20 \log_{10}(185 \text{ deg}/BW_{3\text{dB}})$, following Zimmer et al. (2005).

Ambient noise

Third octave levels (TOLs) of ambient noise were measured on the deepest hydrophone (~ 95 m deep) for both array deployments which contained *Kogia* clicks, as well as on the harbour recordings. Measurements were computed over 1 s analysis windows, in third octave bands centred from 24.8 Hz to 256 kHz, and percentiles (5, 50, 95) within each band were calculated over deployment durations, excluding when the instrument(s) entered and left the water.

Ethics statement

Fieldwork in the Bahamas was conducted under a research permit issued by the Bahamas Department of Marine Resources to BMMRO (no. 12a), under the Bahamas Marine Mammal Protection Act (2005). Recordings in South Africa were made under permit #RES2016/86 (Department of Environmental Affairs) to S.H.E.

RESULTS

Fig. 1 shows a waveform, spectrogram and spectrum from example on-axis *Kogia* clicks. A *Kogia* click, as received on all elements in the array, is also shown (Fig. 2). Spectra of the clicks were stereotyped in frequency and bandwidth (Fig. 3). The clicks recorded on the array were brief ($\sim 142 \pm 37$ μ s; ~ 15 cycles/click) narrow-band pulses (-3 and -10 dB bandwidths of $\sim 4 \pm 2$ kHz and 8 ± 3 kHz, respectively) with high peak frequency (at 123 ± 4 kHz) (Table 1). Localizations of on-axis clicks occurred at a range of 134–718 m, with mean and median depths of 94 and 47 m overlapping with the depth of the array (Table 1). No burst pulses, whistles or buzzes were detected on the array recordings, and no interleaving click trains during either period were observed. The modal ICI was 245 ms (with 5th and 95th percentiles at 55 and 313 ms, respectively) (Fig. 4). On-axis clicks revealed a narrow half-power (-3 dB) beamwidth of 8.8 deg (95% confidence interval, CI, 7.0–10.3 deg), with an equivalent piston radius (EPR) of 4.2 cm (95% CI 3.7–5.5 cm) and a directivity of 27 dB (95% CI 25.2–28.5 dB) (Fig. 5, Table 1). Source parameters are

presented together (Table 1) and also split by observation period (Table S1), to address that a visual confirmation of species ID only existed in period A.

Ranges to on-axis clicks recorded in the harbour averaged 9 ± 7 m (Table 1). A representative click shows that clicks are shorter and contain fewer cycles than the typical click from deep-water recordings (Fig. 1). Spectra of the clicks were also highly stereotyped, with a pronounced shoulder peak frequency at 156 kHz (Fig. 3). The modal ICI (37 ms) was lower than for the deep recordings (Table 1, Fig. 4). Echolocation click trains, closing with buzzes with ICIs as low as 4 ms, were also observed (Fig. 6). Note the varying peak frequency of clicks as the *Kogia* scanned across the recorder (Fig. 6).

In both recording settings, ambient noise in the TOL band (centred at 128 kHz) overlapping with the peak frequency of *Kogia* clicks, was immeasurably quiet, with the 50th percentiles of ambient noise equivalent to the noise floor of the instrument (at ~ 70 – 75 dB re. 1μ Pa, RMS per third octave band) at frequencies >40 kHz (Fig. S2).

DISCUSSION

While the biosonar parameters and echolocation behaviour of most toothed whales, as for bats, conform to scaling predictions from size and broadscale niche segregation (Schnitzler and Kalko, 2001; Jensen et al., 2018), some toothed whales deviate from that general pattern. Here, we investigated one of the prime examples of that, *Kogia*, which are fairly small, yet deep-diving toothed whales that find their deep-sea food by using a high-frequency biosonar system. By using NBHF clicks, half of the power of their biosonar is lost to absorption in <40 m of target range, so how can these cryptic animals find their mesopelagic prey? In this study, we sought to address that question by quantifying the source parameters of *Kogia* echolocation clicks to test the hypotheses that their NBHF clicks are: (i) highly directional; (ii) emitted with long ICIs indicative of relatively longer prey search ranges; and (iii) of a higher SL than shallow diving NBHF species to compensate for the considerable absorption losses of their NBHF clicks.

Directivity

The NBHF clicks of *Kogia* were hypothesized to have a high DI and correspondingly narrow half-power beamwidth, as a result of the short wavelengths of their clicks and the larger aperture of their sound-producing apparatus in their head compared with other NBHF species (Fig. 5). Directionality increases with click frequency and aperture size (Urick, 1983; Madsen and Wahlberg, 2007), and the DI can, for a flat piston, be predicted from $20 \log_{10}(ka)$, where ka is the wavenumber: $2\pi \text{radius}/\lambda$. The *Kogia* melon measures ~ 15 cm in diameter (Clarke, 2003; McKenna et al., 2012), which is roughly twice that of a harbour porpoise (Fig. 5), which produces clicks with similar peak frequency and has a DI of 22–25 dB (Au et al., 1999; Koblitz et al., 2012; Kyhn et al., 2013; Macaulay et al., 2020), suggesting that the DI of *Kogia* should be 6 dB higher. Our piston fitting suggests a DI of 27 dB for the equivalent flat piston aperture diameter of 8.4 cm (Fig. 5). The composite and presumed symmetric beam pattern, with a half-power (-3 dB) beamwidth of 8.8 deg (Fig. 5, Table 1), thus supports our hypothesis of higher directionality than harbour porpoises (at ~ 11 – 13 deg; Koblitz et al., 2012) and other small NBHF species (Jensen et al., 2018), but is not as high as the 28–31 dB predicted from the wavenumber. Our prediction of a higher DI for *Kogia* than for most odontocetes, based on the simple prediction concerning the ratio between the short dominant

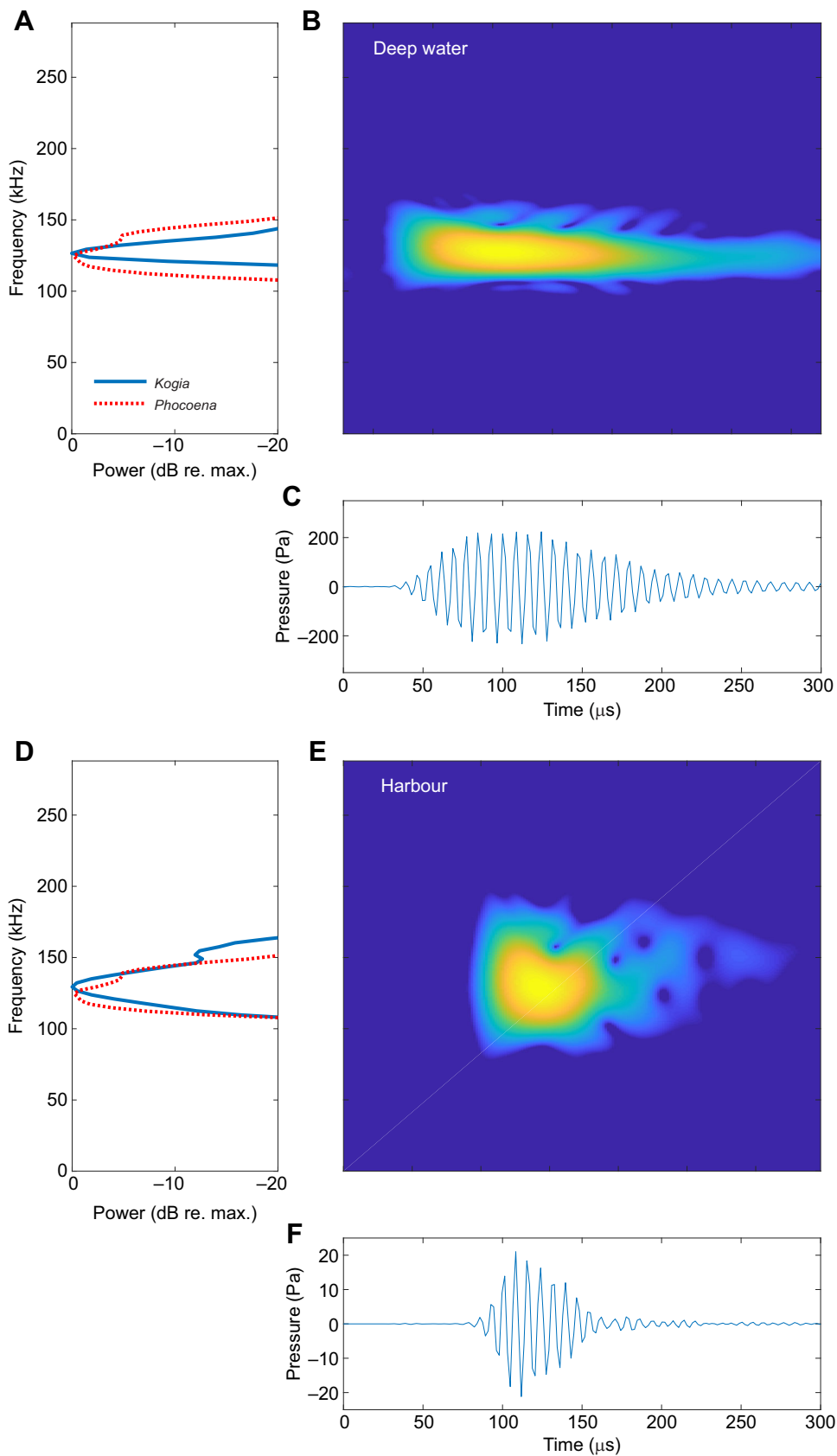


Fig. 1. Representative *Kogia sima* clicks from both recording environments. (A,D) Spectrum, (B,E) spectrogram, and (C,F) source level (SL) of waveform of representative *K. sima* click from deep water (Bahamas, left) and shallow harbour (Cape Town, South Africa, right) recordings (sampling at 576 kHz, FFT size of 2048 for a frequency resolution of 281 Hz). An average normalized spectrum of 65 on-axis harbour porpoise (*Phocoena phocoena*) clicks (from Macaulay et al., 2020, courtesy of J. Macaulay) is superimposed on A and D.

wavelength and larger head size (*sensu* Au et al., 1999), is therefore not supported by the composite beam pattern (Fig. 6). However, the composite DI of 27 dB matches well with the mean observed across

toothed whales, lending support to the notion of a remarkable convergence on click directionality across echolocating toothed whales (Jensen et al., 2018), with smaller odontocetes producing

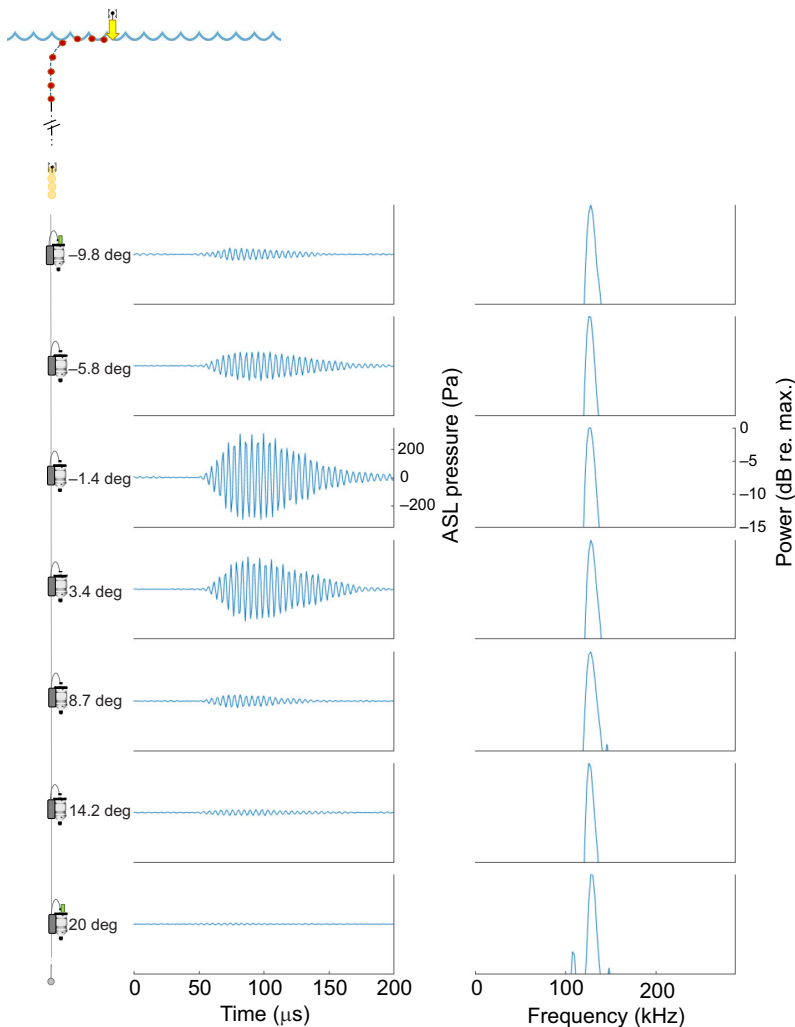


Fig. 2. Sample *K. sima* click recorded on all channels of the vertical hydrophone array. Waveform [apparent source level (ASL) pressure] and normalized power spectra of a representative on-axis *Kogia* click detected on all array elements. The angle indicates where the localization was relative to where the biosonar beam was pointing along the array.

clicks with higher frequencies to achieve the same acoustic field of view. The directional biosonar beam provides a narrow acoustic field of view, allowing for higher SLs and greater on-axis detection range, while facilitating the reduction of acoustic clutter through spatial filtering of off-axis echoes (Au, 1993; Moss and Surlykke, 2001; Jensen et al., 2018).

Despite *Kogia*'s larger head than other NBHF species, the surface through which sound exits the *Kogia* forehead over the melon (the 'oval face') is relatively narrow and flat (Goold and Clarke, 2000), and is comparable with the size of the derived equivalent piston radius (Fig. 5, Table 1; Clarke, 2003). Thus, it may be speculated that the anteriorly tapered melon of the *Kogia*, which is much narrower than the head itself (Fig. 5, inset), may have evolved to form an average acoustic field of view of around 9 deg to offer a balance between clutter rejection and acoustic field of view, as in most other toothed whales (Jensen et al., 2018). Some data points, however, in the radiation pattern of Fig. 5, imply that some *Kogia* NBHF clicks have a half-power beamwidth that is about half or double the mean (of 8.8 deg), suggesting that *Kogia*, similar to porpoises (Wisniewska et al., 2015), can potentially change the width of their sonar beam by changing the effective radiating aperture. Such adjustments are in addition to the demonstrated flexibility in click bandwidth observed in the shallow and deep-water recordings (Figs 1 and 2, Table 1). The complex sound-producing nasal structures of *Kogia*, with a single large phonic lip

pair, intricately shaped air sacs, and a spermaceti organ preceding the melon (Clarke, 2003; Bloodworth and Odell, 2008; McKenna et al., 2012; Thornton et al., 2015), certainly offer the biomechanical potential for such changes in the degree of collimation (e.g. Au et al., 2006), as well as the possibility of the *Kogia* beam being asymmetric. Additionally, because the *Kogia* skull is canted downward (McKenna et al., 2012), it is possible that the beam is transmitted in a downwards direction, as has been found for biosonar beams radiating from Risso's dolphins (Philips et al., 2003). These hypotheses can potentially be tested on *Kogia* in rehabilitation to further our understanding of beam angles and biosonar-guided functional feeding morphology.

ICIs and inferred inspection ranges

Echolocators generally wait for the return of echoes of interest prior to emitting the next click, and ICI can therefore serve as a proxy for the maximum range an echolocating animal is expecting echoes of interest, the so-called inspection range (e.g. Au et al., 1974; Kadane and Penner, 1983; Akamatsu et al., 2005). From their deep-water food niche, we predicted *Kogia* would use ICIs longer than those of other NBHF toothed whales, to reflect longer-range biosonar-mediated foraging and navigation in the open ocean. The harbour porpoise, for example, has, on average, ICIs between 40 and 60 ms in the search phase of biosonar-based hunting (Villadsgaard et al., 2007; Verfuß et al., 2009; Fig. 4C). With a median ICI of 228 ms in

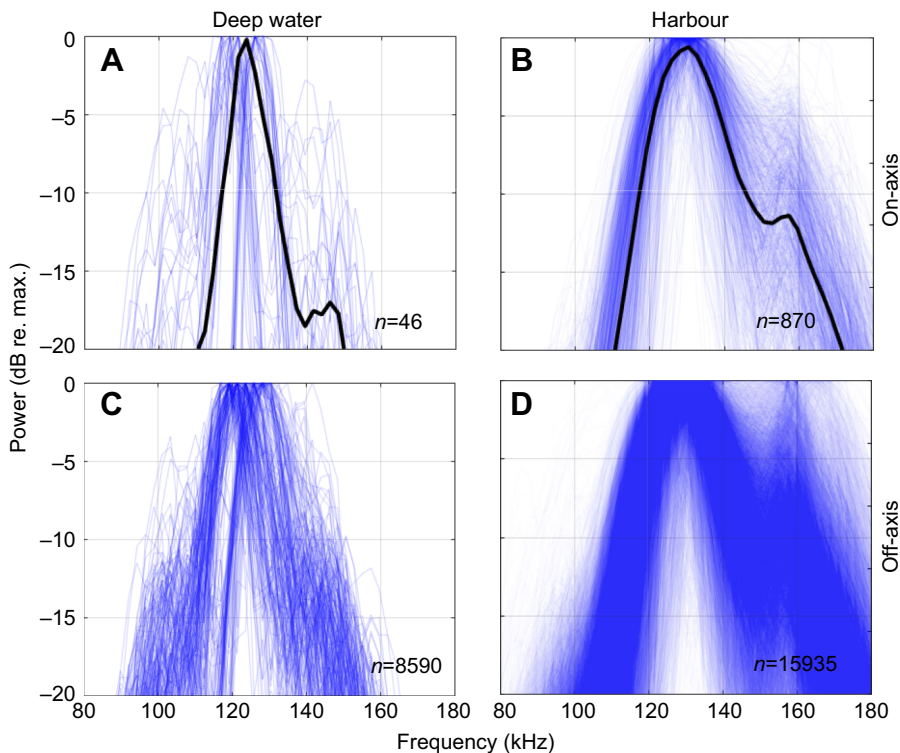


Fig. 3. Spectra of *K. sima* clicks. Clicks are shown from array recordings in the Bahamas (A,C) and single-channel recordings from Cape Town harbour, South Africa (B,D), separated into on-axis (A,B) and off-axis (C,D) clicks. Average spectra are shown as a black line for on-axis clicks.

deep water (Table 1, Fig. 4A), our data are consistent with the hypothesis that *Kogia* employ a longer inspection range (Fig. 4). The majority of *Kogia* ICIs in deep water are about 3–4 times longer than those of NBHF species in shallow water, including *Kogia* in shallow water (Fig. 4B), harbour porpoises (Fig. 4C) and *Cephalorhynchus* (Leeney et al., 2011), suggesting an inspection range that is ~150 m longer. Alternatively, the long ICIs may be an upper bound on the time after each click at which reverberation from multiple scatters, on average, has faded enough to avoid interfering with the next click–echo pair and cause range ambiguity problems. Other deep-diving toothed whales, such as beaked whales, sperm whales and Risso’s dolphins, also have long ICIs that suggest the perceptual organization of a long-range, complex multi-target environment is aided by avoiding range ambiguity (Madsen et al., 2005b, 2013; Fais et al., 2016; Jensen et al., 2020).

However, the long ICIs in *Kogia* are not hard-wired: the relatively long median ICI of >200 ms is over twice the ICI of *Kogia* observed by PAM in deep-water environments (e.g. Merkens et al., 2018; Merkens and Oleson, 2018; Hodge et al., 2018; Hildebrand et al., 2019). Note that the secondary peak in the ICI histogram (Fig. 4A) at ~125 ms corresponds with ICIs from free-ranging *Kogia sima* reported by Merkens et al. (2018). Additionally, the harbour recordings demonstrate that this deep-water species, like other NBHF species (Ladegaard and Madsen, 2019) and bats (Surlykke and Moss, 2000), can adjust its biosonar behaviour to the conditions of the habitat, by emitting clicks with shorter ICIs in keeping with likely shorter ranges of inspection (Fig. 4). Shallow-water recordings in the harbour had ICIs comparable to those of porpoises (mode of 38 ms; Table 1, Fig. 4), indicating a maximum biosonar inspection range of ~30 m. Furthermore, the ICIs of the *Kogia sima* recorded in the shallow harbour (51 ± 34 ms; Table 1) overlap with the ICIs from a *Kogia breviceps* recorded in a shallow, concrete pool (40–70 ms; Madsen et al., 2005a). These are probably habitat-related adjustments in overall acoustic gaze.

Such adjustments in ICI and inspection range take their most extreme form in the buzz, where clicks with short ICIs serve the apparently ubiquitous role among toothed whales of providing high-resolution biosonar updates of a small auditory scene during the final phases of prey target interception (Madsen and Surlykke, 2013). Buzzes have not previously been reported for *Kogia*, with a lowest reported ICI of 25 ms (Merkens et al., 2018) exceeding the ICIs used for defining buzzing of $\sim < 15$ ms for porpoise (DeRuiter et al., 2009; Wisniewska et al., 2014). It therefore begged the question of whether *Kogia* buzz at all, or whether they have simply not been recorded because of the weaker buzz click SLs. While no buzzes were recorded on the deep-water array recordings, with lowest ICIs of 23 ms (Table 1), the harbour recordings contained some echolocation buzzes during close range encounters, using the same sound recorder as the deep-water recordings, with ICIs as low as 4 ms (Table 1, Fig. 6). This buzzing click rate is comparable to those reported in porpoises (Wisniewska et al., 2012; DeRuiter et al., 2009) and dolphins (Wisniewska et al., 2014; Ladegaard et al., 2015; Martin et al., 2018). The pattern of buzzing initiated at a range of around 1–2 body lengths from a prey item appears consistent across a broad range of sizes of toothed whales, from large sperm whales (Fais et al., 2016; Tønnesen et al., 2020) and Blainville’s beaked whales (Johnson et al., 2008) to porpoises (Wisniewska et al., 2012), and appears to be in agreement with the buzzing *Kogia sima* presented here. These ‘hand-off distances’ – from an approach phase to a buzzing interception phase – seem, along with maximum clicks rates, to be scaled with the whale’s size and manoeuvrability (Madsen et al., 2013). Interestingly, the single phonic lip pair of the *Kogia* is large (1.8–3.8 cm; Thornton et al., 2015) compared with that of a harbour porpoise (0.8–1.3 cm; Huggenberger et al., 2009), and yet they can support fast click rates (Fig. 5, Table 1) of similar NBHF clicks (Fig. 1), highlighting both the difficulty of inferring acoustic outputs from anatomy and that much remains to be understood regarding the biomechanical details of pneumatic sound production in odontocetes.

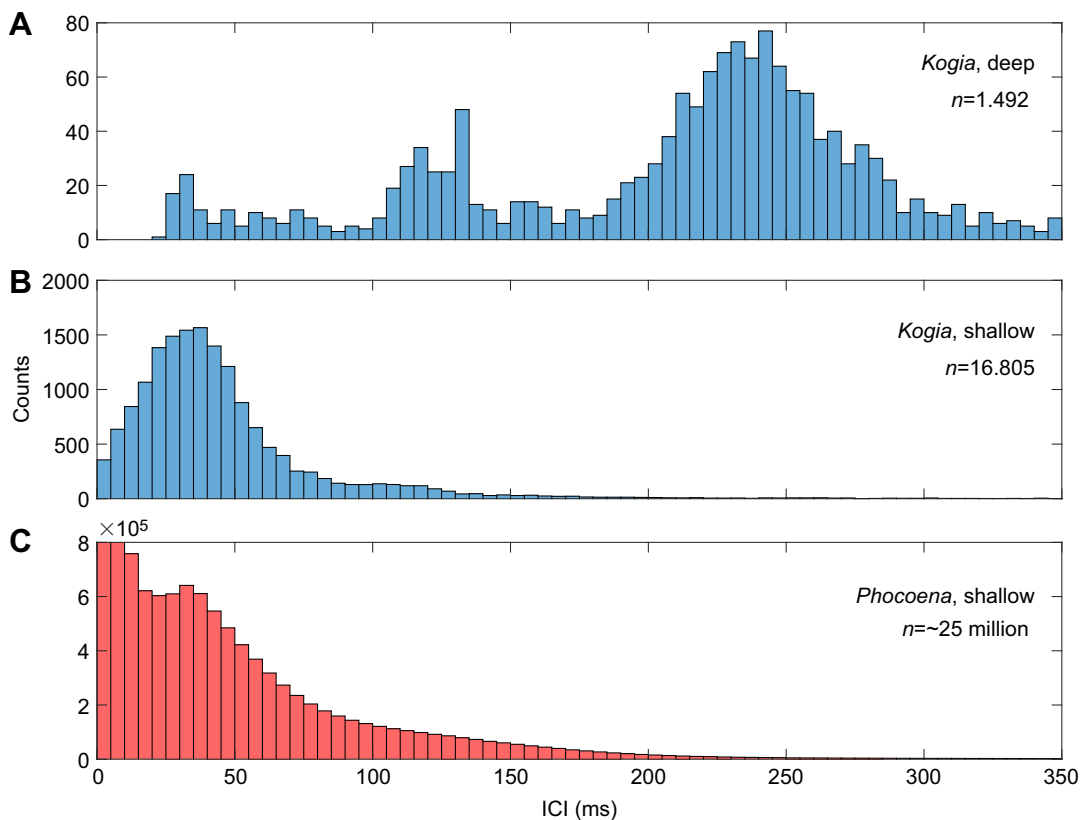


Fig. 4. Inter-click interval comparison. Inter-click intervals (ICIs; 5 ms bins) of narrow-band high-frequency (NBHF) toothed whales, as derived from on- and off-axis recordings of clicks. (A) *Kogia sima* recorded in deep water, Bahamas. (B) *Kogia sima* recorded in the shallow harbour, South Africa. (C) Data from 19 *P. phocoena* sound-and-movement tag recordings in shallow coastal Danish waters (courtesy of L. Rojano-Doñate). Note that y-axis is zoomed in to highlight non-buzz ICIs.

Source level and biosonar detection ranges

From the consistent observations of deep-water prey in the stomachs of *Kogia*, we hypothesized, like Kyhn et al. (2010), that *Kogia* hunting in the deep should produce higher SLs than shallow-water NBHF species to facilitate prey detection in their vast 3-dimensional foraging habitats. This notion is supported by their significantly longer ICIs than shallow-water NBHF species. Additionally, body size scaling with SL in toothed whales (Jensen et al., 2018) predicts that *Kogia*, with body sizes similar to those of bottlenose dolphins, should be able to produce SLs of more than 220 dB re. $1 \mu\text{Pa}_{\text{pp}}$ (Au et al., 1974). However, the *Kogia* clicks we recorded in the open ocean environment have a mean SL of 186 ± 6 dB re. $1 \mu\text{Pa}_{\text{pp}}$ at 1 m and a maximum of 197 dB re. $1 \mu\text{Pa}_{\text{pp}}$ at 1 m (Table 1). So, in contrast to our predictions and hypothesis, the moderate SLs reported here overlap with the SLs of clicks produced by harbour porpoises in shallow waters, with reported mean SL of ~ 189 – 191 dB re. $1 \mu\text{Pa}_{\text{pp}}$ at 1 m (Villadsgaard et al., 2007; Kyhn et al., 2013; Macaulay, 2020). These results are also at odds with the assumptions of Hildebrand et al. (2019), who used SL estimates of 212 ± 5 dB re. $1 \mu\text{Pa}_{\text{pp}}$ at 1 m to simulate acoustic density estimation of *Kogia*.

It may well be, of course, that we have not captured to the full capability of source outputs from *Kogia* and that they, in some contexts, use higher SLs than recorded here. Such flexibility is exemplified by our finding that the median SL of clicks emitted in the open environment was 28 dB greater than the median SL of those emitted in the harbour (Table 1). In deep water, the *Kogia* clicks were only recorded during two array deployments when the

maximum hydrophone depth was ~ 95 m, and during these periods, *Kogia* were localized to a maximum depth of 392 m (Table 1). As *Kogia* are thought to dive deeper than this, and have been recorded on PAM instruments at depths of ~ 1000 m (Hodge et al., 2018), it is possible that higher SLs are instead employed at greater depths than those we recorded at, or when descending towards the prey layer, during which a vertical array may not receive powerful on-axis clicks. While the majority (69%) of our sampling effort was when the deepest channel on the array was at ~ 300 m, no *Kogia* clicks were recorded on any of these deeper deployments, so perhaps our deployments were not deep enough, or our sampling effort of nearly 75 h was not enough to capture the full SL dynamic range. However, smaller datasets from similar-sized delphinids in oceanic waters consistently return SL estimates between 200 and 220 dB re. $1 \mu\text{Pa}_{\text{pp}}$ at 1 m (e.g. Au et al., 1974; Au and Herzing, 2003; Madsen et al., 2004), much higher than those found here, in turn suggesting that perhaps these low SLs indeed are representative.

So what are the prey detection implications of the moderate SLs documented here? Because the NBHF *Kogia* clicks have durations of ~ 100 – $200 \mu\text{s}$ in deep water (Table 1), they carry some 10 dB more energy for the same peak pressure compared with the short, broadband clicks of many delphinids and river dolphins, and 2–4 dB more energy than typical NBHF clicks of porpoises and dolphins of the *Cephalorhynchus* genus (Kyhn et al., 2009; 2010; Jensen et al., 2018). As the ear operates as an energy detector with a short integration time of around $260 \mu\text{s}$ in small toothed whales (Vel'min and Dubrovsky, 1975; Moore et al., 1984; Au et al., 1988; Supin and Popov, 1995), the appropriate measure for comparatively

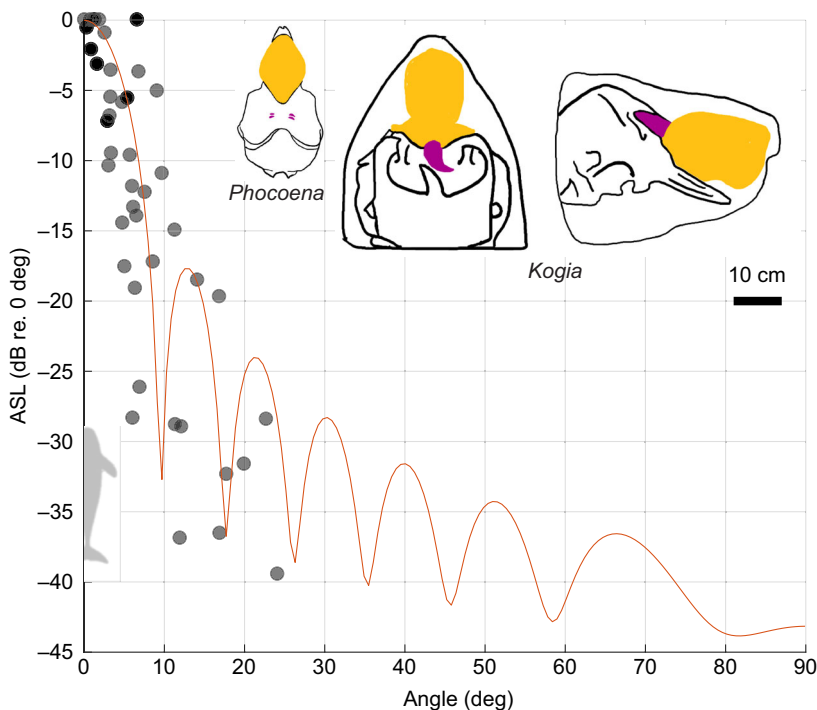


Fig. 5. Beam pattern of on-axis *K. sima* clicks. The line shows the theoretical beam pattern of a 8.4 cm diameter piston transmitting a *Kogia* click, and the dots show the ASL (relative to 0 deg) as a function of receiving angle of incidence for on-axis clicks ($n=21$), with each click contributing at least 3 points. The dots are partially transparent to emphasize that many clicks have half-power beamwidths narrower than the reported overall half-power beamwidth of 8.8 deg. Superimposed images of *Kogia breviceps* melon (adapted from McKenna et al., 2012) and *P. phocoena* melon (adapted from Huggenberger et al., 2009) are inset to emphasize differences in skull and melon sizes between *Kogia* and the harbour porpoise; yellow shows the melon and magenta shows the bursae/spermaceti organ complexes.

evaluating prey detection performance in *Kogia* is therefore not pressure, but rather the EFD (Au, 1993) of the returning echo. Target detection experiments with porpoises (Kastelein et al., 1999; Au et al., 2007) have not provided clear measures of detection threshold (DT) as performance as a function of measured SLs in target detection experiments was not logged. Therefore, we shall assume the DT of ~ 33 dB re. $1 \mu\text{Pa}^2 \text{ s}$, as measured for *Tursiops* during an unmasked detection experiment (Au et al., 2002). If we assume that threshold is valid for *Kogia* also, and assume a target strength (TS) range of ~ -35 to -45 dB of myctophid and cephalopod prey (Benoit-Bird and Au, 2001) typical of *Kogia*, we can, by using the sonar equation (Eqn 1), estimate the range over which they may be able to detect such prey under low-noise, clutter-free conditions with a median SL_{EFD} of 134 dB re. $1 \mu\text{Pa}^2 \text{ s}$ (Table 1):

$$\text{DT} = \text{SL} - 2\text{TL} + \text{TS}. \quad (1)$$

By inserting the relevant numbers (*sensu* Madsen et al., 2007), we find that a *Kogia*, in this scenario, will have ~ 56 – 66 dB available for two-way TL which, under the assumption of spherical spreading and absorption at 125 kHz, corresponds to a maximum detection range of about ~ 23 – 38 m. That TL number will increase to ~ 69 – 79 dB, or some ~ 43 – 68 m of target range if we use the highest measured SL_{EFD} of 147 dB re. $1 \mu\text{Pa}^2 \text{ s}$.

It may well be that *Kogia* have evolved lower detection thresholds than dolphins, owing to their echolocation in a narrow high-frequency bandwidth down to a median of 2 kHz (BW_{RMS} , Table 1) under very low noise levels in the deep sea. We could not reliably measure third octave noise levels at the centre frequency of *Kogia* clicks in the recording habitats because they were consistently below the low self-noise of the SoundTrap recorders (Fig. S2). So, in the absence of actual numbers, we can only say that *Kogia* echolocate under very low noise conditions, perhaps approximated by the Wenz curve minima (Wenz, 1962) in a narrow bandwidth around 125 kHz. If indeed their DT has been shaped evolutionarily

by the lowest ambient noise levels over the click, their DT may be the lowest for any odontocete, including dolphins and porpoises. We propose this by considering two potential sources of gain on the reception side of the biosonar feedback loop: a narrower bandwidth of their click than porpoises, and a narrower receiving DI. Firstly, a mean RMS bandwidth of 2–3 kHz (Table 1) is the narrowest bandwidth of any toothed whale echolocation click on record, 2–3 times narrower than for clicks of other NBHF species, and about 10 times narrower than the clicks of bottlenose dolphins. This reduction in bandwidth could potentially be driving the DT estimate for *Kogia* down by 3–4.5 dB compared with that of a porpoise (Au et al., 2007) and by 10 dB compared with that of a dolphin (Au, 1993), as calculated by $10\log_{10}$ (factor of bandwidth reduction), if matched in narrowness by the auditory filters. Secondly, because the sound-receiving pan bones of the lower jaws in *Kogia*, acting as outer ears, are separated by twice the distance of the pan bones of a porpoise, the ambient noise-suppressing receiving DI is, all other things being equal, expected to be ~ 6 dB better than for a porpoise (of ~ 12 dB; Kastelein et al., 2005), and comparable to that of a bottlenose dolphin (of ~ 18 dB; Au and Moore, 1984) (as calculated by $20\log_{10}2$). Combining these two potential noise suppressors, the DT of *Kogia* could be ~ 10 dB lower than that of a dolphin, so that it is instead ~ 23 dB re. $1 \mu\text{Pa}^2 \text{ s}$. Thus, on purely physical grounds, it may be speculated that the DT of a *Kogia* is the lowest among all toothed whales. When assuming this and using, for example, the high SL_{pp} expected by Hildebrand et al. (2019) of 212 dB re. $1 \mu\text{Pa}_{\text{pp}}$ at 1 m, corresponding to a SL_{EFD} of ~ 163 dB re. $1 \mu\text{Pa}^2 \text{ s}$, there is still, under these very ideal and probably unrealistic scenarios, ~ 100 dB available for two-way TL, corresponding to a ~ 155 m target range. Thus, our hypothesis that *Kogia* use high SLs for long-range echolocation of single prey is only tenuously supported: even under the best of scenarios, it is unlikely that *Kogia* detect their preferred prey at the ranges of 150 to 200 m inferred from their long ICIs, but are more likely to employ detection ranges in the tens of metres, on a par with other NBHF species. However, the long ICIs at moderate SLs will allow *Kogia* to

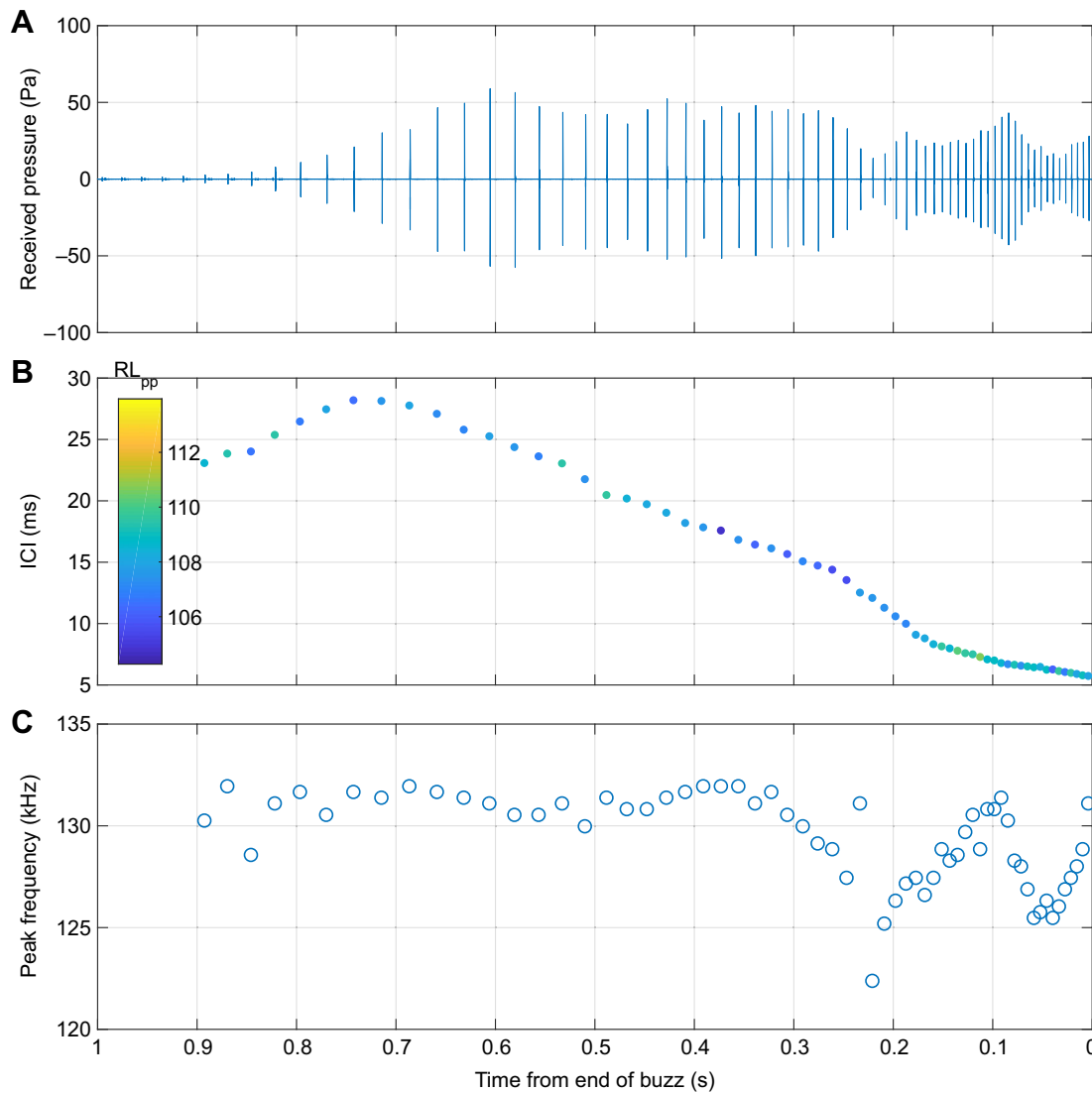


Fig. 6. *Kogia sima* buzz example. (A) Waveform, (B) ICI coloured by peak-to-peak received level (RL_{pp}) and (C) peak frequency displays of an example echolocation sequence ending with a buzz (down to 5.7 ms in this example), from a *K. sima* at a range of 9 m, from the single-channel, close-range harbour recording.

locate the deep scattering layer with volume scattering properties that allow for detection at much longer ranges than its single constituents (Wiebe et al., 1990). Further, in the deep scattering layer, many organisms are schooling (Madsen et al., 2013; Johnson et al., 2008; Benoit-Bird et al., 2017). In concert, these offer the means for a combined higher TS at long ranges, or, if prey schools are large enough relative to ensonification range, will also act as volume scatterers to enable detection ranges in keeping with the long *Kogia* ICIs.

A similar decoupling between long inferred inspection ranges from ICI and moderate calculated biosonar detection ranges of single prey is seen in Blainville's beaked whales, which are proposed to maintain a broad auditory scene via clicking at a low rate (Johnson et al., 2006, 2008). It may thus similarly be speculated that *Kogia* use long ICIs to facilitate auditory streaming of the complex auditory scene generated by a densely packed prey layer in the deep scattering layer, so that most echoes are allowed to return before emission of the next click to avoid range ambiguity problems. Indeed, the complexity of interpreting the acoustic

scene of a scattering layer is acknowledged by how difficult it is for echosounders to register individual animals when echo density is high (Madsen et al., 2005b; Benoit-Bird, 2014).

Benthic species and cephalopods that undergo diel migrations have been found in the stomachs of stranded *Kogia*, with a diet that is largely composed of prey inhabiting the epipelagic (0–200 m) and mesopelagic (~200–1000 m) zones (Plön, 2004; Beatson, 2007). The two species of *Kogia* are understood to have similar foraging ecologies and occupy similar trophic niches (Staudinger et al., 2014). It is therefore plausible that *Kogia* – contrary to their large relative the sperm whale, which has a long-range biosonar – generally forage in slope habitats where they can reliably expect to encounter prey by diving down and then use a short-range biosonar with moderate SLs to hunt once in the prey layer. This notion is reinforced by *Kogia* being a relatively small odontocete and therefore physiologically constrained to shorter duration dives, as has been observed with maximum dive durations around 18–25 min (Breese and Tershy, 1993; Willis and Baird, 1998; Scott et al., 2001). If they are hunting at depth in a narrow time frame, they must

be efficient at doing so, and a predictable prey niche would facilitate this, perhaps limiting the habitats that will support *Kogia*.

Arranz et al. (2011) suggested that as Blainville's beaked whales only start echolocating once they are in a deep scattering layer, there is probably reliability in exploiting prey in that strata. Thus, the predictability in the depth of deep scattering layers (as a function of daylight) allows for a hunting strategy involving low SL echolocation. In the same location south of Abaco Island, Bahamas, where our array was deployed, the surface and deep scattering layers have been investigated using a combination of net tows and active acoustics. Here, intense surface and diffuse deep scattering layers were identified at depths of ~120 and ~540 m, respectively, during the daytime, becoming more intense and migrating shallower at night (Sato and Benoit-Bird, 2017). Our sampling location has been identified as a high-quality foraging habitat for odontocetes, with high density in mesopelagic scattering layers at ~150 and ~700–800 m (Benoit-Bird et al., 2020). Thus, the depths of both our array and the majority of our *Kogia* localizations (Table 1) overlap with scattering layers at this location, supporting our hypothesis that they are foraging in acoustically cluttered prey layers.

Why are *Kogia* clicks so narrowband?

The NBHF click, which convergently evolved in the Phocoenidae, and in the genera *Kogia* and *Cephalorhynchus*, and some dolphins in *Lagenorhynchus* (Kyhn et al., 2009, 2010, 2013; Götz et al., 2010; Reyes Reyes et al., 2016; Bassett et al., 2009; Griffiths et al., 2020), has been hypothesized to have evolved as an adaptation both to take advantage of low ambient noise levels in the ocean at these frequencies and to reduce acoustic detectability by predators (Møhl and Andersen, 1973; Andersen and Amundin, 1976; Madsen et al., 2005a; Morisaka and Connor, 2007; Kyhn et al., 2013). While predatory killer whales (and perhaps also extinct raptorial sperm whales; Galatius et al., 2019) may still be able to hear porpoise clicks, their hearing is much less sensitive at >100 kHz (Hall and Johnson, 1972; Szymanski et al., 1999; Branstetter et al., 2017). If correct, such acoustic crypsis comes at the cost of high levels of frequency-dependent absorption and hence inherently low sonar ranges. Here, we have shown that *Kogia* address the challenge of echolocating to find prey in the deep while possibly evading acoustic detection by predators by producing clicks with a high DI, narrow frequency bandwidth, moderate SL and surprisingly long ICIs. Our observation that *Kogia* click near the surface when in deep-water environments, and that all clicks were >100 kHz (Table 1), is consistent with the acoustic crypsis hypothesis. Beaked whales, in contrast, emit lower-frequency clicks audible to killer whales, avoid clicking in depths shallower than 300 m, and surface in silence well away from where their last clicks were made (Aguilar de Soto et al., 2020). Thus, *Kogia* seem to navigate 'soundscapes of fear' differently from beaked whales, enabling them to vocalize more safely in shallower depths. The production of lower-frequency clicks by NBHF-producing Heaviside's dolphins in a conspecific communication context emphasizes the trade-off in communication range versus acoustic detection by predators (Martin et al., 2018). Predation by killer whales in the same location in which our array recordings were made (Dunphy-Daly et al., 2008; Dunn and Claridge, 2014) highlights that predation risks posed by killer whales are real and supports the notion of predation as a driver of acoustic crypsis. Even in light of updated killer whale audiograms (Branstetter et al., 2017), acoustic crypsis of *Kogia* clicks is still provided spatially via absorption, if not spectrally via overlap with a predator's auditory sensitivity.

Another notion to entertain, given their long click duration and extremely narrow bandwidth, is whether the *Kogia* biosonar system is sensitive to and makes use of Doppler shifts in the echoes of moving prey to facilitate acoustic localization, as is the case for some bats (Schnitzler, 1973). However, given the 4.5 times greater sound speed in water than in air, combined with the high frequency of *Kogia* clicks, a reasonable escape speed of a prey item of ~1.5 m s⁻¹ would yield a Doppler shift of only ~250 Hz, which is very small given the 2–10 kHz bandwidth of their clicks (Table 1) and the 10 kHz variation in the centre frequency, leading us to conclude that echolocation using NBHF clicks is insensitive to realistic Doppler shifts (*sensu* Madsen et al., 2005a). With the long click duration comes a narrower bandwidth, and while this provides poorer range resolution than would a broadband click (Møhl and Andersen, 1973), target detection capabilities improve because the echo energy arrives in a narrower frequency band with less noise compared with the same energy distributed over a broader band (Madsen et al., 2005a). Given the highly selective foraging behaviour documented for Blainville's beaked whales (Madsen et al., 2005b; Arranz et al., 2011), it also remains an open question of how *Kogia* may perform target discrimination with a narrow-band click carrying less information about target properties than a broadband click.

Furthermore, we argue that a click of extremely narrow bandwidth would evolve in parallel with an equally narrow auditory filter matched with the high Q of their signal (mean of 56; Table 1, Figs 1 and 3). Indeed, if the auditory filter is wider in bandwidth, noise in frequencies outside the click bandwidth will contribute unnecessary masking effects. Additionally, the frequency range of the most sensitive hearing in odontocetes is generally around the average frequency of the echolocation signals (Kastelein et al., 2002), so an auditory filter matched in bandwidth to the resonant quality factor of clicks gives the best trade-off between time and frequency resolutions of the returning echoes. The hypothesis of a narrow auditory filter in *Kogia*, proposed by Madsen et al. (2005a), is consistent with anatomical inference of ganglion density in the cochlea located in the NBHF frequency region in *Phocoena* (Ketten, 2000), and by auditory brainstem evoked potential studies (Ridgway and Carder, 2001). This hypothesis could be tested by measuring the *Kogia* acoustic fovea and critical bandwidth on an animal in rehabilitation using non-invasive evoked potential techniques.

Applied implications

Here, the click parameter quantification from close-range and species-identified *Kogia* contributes to a growing body of PAM literature on this genus. Our findings on the relative stereotypy of their clicks make them a good candidate for PAM to study their presence, distribution, density and relative abundance (Hildebrand et al., 2019). Effective PAM relies on species-specific bioacoustic quantifications for classification (Zimmer, 2011; Baumann-Pickering et al., 2013) and is a critical first step for management recommendations and conservation. Confidence in acoustic ID is becoming increasingly relevant for automated processing as PAM equipment becomes cheaper and more accessible, as high-bandwidth and longer-term datasets become more common, and as acoustic monitoring methods become more autonomous (e.g. Gkikopoulou, 2018). Our quantifications are potentially useful for acoustically discriminating between *Kogia* species, which broadly overlap in distribution and are currently considered acoustically indistinguishable (Merkens et al., 2018), and for discriminating them from other, sometimes sympatric, NBHF species (see Griffiths et al., 2020). Source parameters and the beam pattern have recently

been used to estimate acoustic detection probabilities and inform density estimation in long-term datasets (Frasier et al., 2016; Hildebrand et al., 2019).

Given the high absorption (~ 40 dB/km) of NBHF clicks, the median ASL from the array recordings of 186 dB re. $1 \mu\text{Pa}_{\text{pp}}$ at 1 m (Table 1), and assuming a typical modest detection threshold of 110 dB re. $1 \mu\text{Pa}_{\text{pp}}$, we calculate a maximum passive acoustic detection range of ~ 450 m. Even at the highest recorded ASL (of 197 dB re. $1 \mu\text{Pa}_{\text{pp}}$ at 1 m), the maximum range at which a *Kogia* click exceeds the acoustic detection threshold is only ~ 750 m. Thus, while it has been noted that *Kogia* presence is underestimated in visual surveys (Barlow, 1999; Hodge et al., 2018), their presence could also be underestimated in PAM surveys if the acoustic detection probability (g_0) assumes a greater SL, and as they are only detectable at ranges of less than 1 km, even under ideal conditions.

A handful of clicks with lower peak frequencies (< 120 kHz) were observed here in both datasets (Fig. 3). Similar variations in *Kogia* peak frequency have been observed by others (Merkens et al., 2018; Merkens and Oleson, 2018; Hildebrand et al., 2019; Griffiths et al., 2020). Indeed, there is similar variation of ~ 12 kHz in the F_p of harbour porpoise clicks (Kyhn et al., 2013). Varying F_p has been found within *Kogia* click train events (Merkens et al., 2018; Griffiths et al., 2020), and is similarly shown here with F_p variation coinciding with RL variation (Fig. 6). As period B of the array recordings had no visual observation of any odontocete, it could have instead recorded the sounds of *Kogia breviceps* (Cardona-Maldonado and Mignucci-Giannoni, 1999; Dunn and Claridge, 2014), which is less commonly observed in the Bahamas. It is possible that variations in our measurements are due to undescribed acoustic differences between the two species, but similarity across acoustic parameters of on-axis clicks from both periods A and B suggests that the two recordings are from the same species, *Kogia sima* (Table S1).

Conclusion

Here, we have measured the source parameters of NBHF echolocation clicks produced by free-ranging *Kogia* recorded in deep- and shallow-water settings. While such clicks are subject to significant levels of frequency-dependent absorption losses, these whales successfully find their mesopelagic prey by producing clicks that are highly directional and extremely narrowband to hunt in the predictable layers of aggregated prey at depth. Their SLs were lower than expected, but the suggested gains in their auditory detection threshold could partially compensate for the short ranges that their low output levels beget. By comparing clicks produced by the same species in different habitats, we have demonstrated flexibility in their output levels and ICIs, and have suggested flexibility in their beamwidth to offer dynamic sensing tailored to the biosonar tasks at hand.

Acknowledgements

Many thanks to the several researchers who generously lent us their SoundTraps: Jonas Teilmann, Magnus Wahlberg, Natacha Aguilar de Soto and Jakob Tougaard. Thanks to the Zoophysiology workshop at Aarhus University (Niels Kristiansen, John Svane Jensen, Mehran Jahanara and Lasse Vestergaard Sørensen) for preparing trawl floats and designing the 3D-printed moulds used as breakouts in the vertical array. Thanks to Magnus Wahlberg for helpful comments on the initial results, Kristian Beedholm for help with the piston model, and Michael Ladegaard for assistance with click parameterization. Thanks to Jamie Macaulay for providing example on-axis harbour porpoise clicks, and to Laia Rojano-Doñate for providing click data from a dataset of 19 wild, tagged porpoises in Danish waters. Finally, many thanks to the two anonymous reviewers who found the time during a pandemic to provide helpful suggestions on an earlier version of the manuscript.

Competing interests

The authors declare no competing or financial interests.

Author contributions

Conceptualization: C.E.M., P.T.M.; Methodology: C.E.M., P.T.M.; Software: C.E.M.; Validation: C.E.M.; Formal analysis: C.E.M.; Investigation: C.E.M., P.T., C.A.D., D.E.C., T.G., S.H.E., P.T.M.; Resources: C.A.D., D.E.C., T.G., S.H.E., P.T.M.; Data curation: C.E.M.; Writing - original draft: C.E.M., P.T.M.; Writing - review & editing: C.E.M., P.T., C.A.D., D.E.C., T.G., S.H.E., P.T.M.; Visualization: C.E.M.; Supervision: P.T.M.; Project administration: C.E.M., P.T.M.; Funding acquisition: C.E.M., P.T.M.

Funding

PhD and fieldwork funding were provided by the Danmarks Grundforskningsfond (27125 to P.T.M.), the Oticon Fonden (18-0340 to C.E.M.) the Dansk Akustisk Selskab (to C.E.M.), the South Africa National Research Foundation (research career advancement fellowship to S.E.) and the Claude Leon Foundation (postdoctoral fellowship to T.G.).

Data availability

The PAMGuard data analysis software is open source and available at: <https://sourceforge.net/p/pamguard/svn/HEAD/tree/PamguardJava/>. The compiled software is available at: www.pamguard.org. The dataset of on-axis clicks, used for source parameter quantification, is available from Zenodo to facilitate the training of automated click classifiers: doi.org/10.5281/zenodo.4273697. This includes sound clips of all of the on- and off-axis *Kogia sima* clicks, and calculated localization ranges and off-axis angles.

Supplementary information

Supplementary information available online at <https://jeb.biologists.org/lookup/doi/10.1242/jeb.240689.supplemental>

References

- Aguilar de Soto, N., Johnson, M. P., Madsen, P. T., Díaz, F., Domínguez, I., Brito, A. and Tyack, P. (2008). Cheetahs of the deep sea: deep foraging sprints in short-finned pilot whales off Tenerife (Canary Islands). *J. Anim. Ecol.* **77**, 936-947. doi:10.1111/j.1365-2656.2008.01393.x
- Aguilar de Soto, N., Visser, F., Tyack, P. L., Alcazar, J., Ruxton, G., Arranz, P., Madsen, P. T. and Johnson, M. (2020). Fear of killer whales drives extreme synchrony in deep diving beaked whales. *Sci. Rep.* **10**, 13. doi:10.1038/s41598-019-55911-3
- Ainslie, M. A. and McCole, J. G. (1998). A simplified formula for viscous and chemical absorption in sea water. *J. Acoust. Soc. Am.* **103**, 1671-1672. doi:10.1121/1.421258
- Akamatsu, T., Wang, D., Wang, K. and Naito, Y. (2005). Biosonar behaviour of free-ranging porpoises. *Proc Roy Soc B* **272**, 797-801. doi:10.1098/rspb.2004.3024
- Andersen, S. and Amundin, M. (1976). Possible predator-related adaption of sound production and hearing in the harbour porpoise (*Phocoena phocoena*). *Aquat. Mamm.* **4**, 56-58.
- Arranz, P., Aguilar de Soto, N., Madsen, P. T., Brito, A., Bordes, F. and Johnson, M. P. (2011). Following a foraging fish-finder: diel habitat use of Blainville's beaked whales revealed by echolocation. *PLoS ONE* **6**, e28353. doi:10.1371/journal.pone.0028353
- Au, W. W. L. (1993). *The Sonar of Dolphins*. New York, USA: Springer-Verlag.
- Au, W. W. L. and Herzog, D. L. (2003). Echolocation signals of wild Atlantic spotted dolphin (*Stenella frontalis*). *J. Acoust. Soc. Am.* **113**, 598-604. doi:10.1121/1.1518980
- Au, W. W. L. and Moore, P. W. (1984). Receiving beam patterns and directivity indices of the Atlantic bottlenose dolphin *Tursiops truncatus*. *J. Acoust. Soc. Am.* **75**, 255-262. doi:10.1121/1.390403
- Au, W. W. L., Floyd, R. W., Penner, R. H. and Murchison, A. E. (1974). Measurement of echolocation signals of the Atlantic bottlenose dolphin, *Tursiops truncatus* Montagu, in open waters. *J. Acoust. Soc. Am.* **56**, 1280-1290. doi:10.1121/1.1903419
- Au, W. W. L., Floyd, R. W. and Haun, J. E. (1978). Propagation of Atlantic bottlenose dolphin echolocation signals. *J. Acoust. Soc. Am.* **64**, 411-422. doi:10.1121/1.382015
- Au, W. W. L., Penner, R. H. and Turl, C. W. (1987). Propagation of beluga echolocation signals. *J. Acoust. Soc. Am.* **82**, 807-813. doi:10.1121/1.395278
- Au, W. W. L., Moore, P. W. and Pawloski, D. A. (1988). Detection of complex echoes in noise by an echolocating dolphin. *J. Acoust. Soc. Am.* **83**, 662-668. doi:10.1121/1.396161
- Au, W. W. L., Kastelein, R. A., Rippe, T. and Schooneman, N. M. (1999). Transmission beam pattern and echolocation signals of a harbor porpoise (*Phocoena phocoena*). *J. Acoust. Soc. Am.* **106**, 3699-3705. doi:10.1121/1.428221
- Au, W. W. L., Lemonds, D. W., Vlachos, S., Nachtigall, P. E. and Roitblat, H. L. (2002). Atlantic bottlenose dolphin (*Tursiops truncatus*) hearing threshold for brief broadband signals. *J. Comp. Psych.* **116**, 151-157. doi:10.1037/0735-7036.116.2.151

- Au, W. W. L., Kastelein, R. A., Benoit-Bird, K. J., Cranford, T. W. and McKenna, M. F.** (2006). Acoustic radiation from the head of echolocating harbor porpoises (*Phocoena phocoena*). *J. Exp. Biol.* **209**, 2726–2733. doi:10.1242/jeb.02306
- Au, W. W. L., Benoit-Bird, K. J. and Kastelein, R. A.** (2007). Modeling the detection range of fish by echolocating bottlenose dolphins and harbor porpoises. *J. Acoust. Soc. Am.* **121**, 3954–3962. doi:10.1121/1.2734487
- Barlow, J.** (1999). Trackline detection probability for long-diving whales. In *Marine Mammal Survey and Assessment Methods* (ed. G. W. Garner, S. C. Ampstrup, J. L. Laake, B. F. J. Manly, L. L. McDonald and D. G. Robertson), pp. 209–221. Rotterdam, The Netherlands: Balkema Press.
- Bassett, H. R., Baumann, S., Campbell, G. S., Wiggins, S. M. and Hildebrand, J. A.** (2009). Dall's porpoise (*Phocoenoides dalli*) echolocation click spectral structure. *J. Acoust. Soc. Am.* **125**, 2677–2677. doi:10.1121/1.4784219
- Baumann-Pickering, S., McDonald, M. A., Simonis, A. E., Solsona Berga, A., Merkens, K. P., Oleson, E. M., Roch, M. A., Wiggins, S. M., Rankin, S. and Yack, T. M.** (2013). Species-specific beaked whale echolocation signals. *J. Acoust. Soc. Am.* **134**, 2293–2301. doi:10.1121/1.4817832
- Baumgartner, M. F., Mullin, K. D., May, L. N. and Leming, T. D.** (2001). Cetacean habitats in the northern Gulf of Mexico. *Fish. Bull.* **99**, 219–219.
- Beatson, E.** (2007). The diet of pygmy sperm whales, *Kogia breviceps*, stranded in New Zealand: implications for conservation. *Rev. Fish. Biol. Fisheries.* **17**, 295–303. doi:10.1007/s11160-007-9039-9
- Beedholm, K. and Møhl, B.** (2006). Directionality of sperm whale sonar clicks and its relation to piston radiation theory. *J. Acoust. Soc. Am.* **119**, EL14–EL19. doi:10.1121/1.2161799
- Benoit-Bird, K. J.** (2014). Deep-diving autonomous underwater vehicle provides insights into scattering layer dynamics. *J. Acoust. Soc. Am.* **135**, 2154–2154. doi:10.1121/1.4876983
- Benoit-Bird, K. J. and Au, W. W.** (2001). Target strength measurements of Hawaiian mesopelagic boundary community animals. *J. Acoust. Soc. Am.* **110**, 812–819. doi:10.1121/1.1382620
- Benoit-Bird, K. J., Moline, M. A. and Southall, B. L.** (2017). Prey in oceanic sound scattering layers organize to get a little help from their friends. *Limnol. Oceanogr.* **62**, 2788–2798. doi:10.1002/lno.10606
- Benoit-Bird, K. J., Southall, B. L., Moline, M. A., Claridge, D. E., Dunn, C., Dolan, K. A. and Moretti, D. J.** (2020). Critical threshold identified in the functional relationship between beaked whales and their prey. *Mar. Ecol. Prog. Ser.* **654**, 1–16. doi:10.3354/meps13521
- Bloodworth, B. E. and Odell, D. K.** (2008). *Kogia breviceps* (Cetacea: Kogiidae). *Mamm. Species* **819**, 1–12. doi:10.1644/819.1
- Branstetter, B. K., Leger, J. S., Acton, D., Stewart, J., Houser, D., Finneran, J. J. and Jenkins, K.** (2017). Killer whale (*Orcinus orca*) behavioral audiograms. *J. Acoust. Soc. Am.* **141**, 2387–2398. doi:10.1121/1.4979116
- Breese, D. and Tershy, B. R.** (1993). Relative abundance of Cetacea in the Canal de Ballenas, Gulf of California. *Mar. Mamm. Sci.* **9**, 319–324. doi:10.1111/j.1748-7692.1993.tb00460.x
- Caldwell, D. K. and Caldwell, M. C.** (1989). Pygmy sperm whale *Kogia breviceps* (de Blainville, 1838): dwarf sperm whale *Kogia sima* (Owen, 1866). In *Handbook of Marine Mammals* (ed. S. Ridgway and R. Harrison), pp. 235–260. San Diego, USA: Academic Press.
- Cardona-Maldonado, M. A. and Mignucci-Giannoni, A. A.** (1999). Pygmy and dwarf sperm whales in Puerto Rico and the Virgin Islands, with a review of *Kogia* in the Caribbean. *Caribb. J. Sci.* **35**, 29–37.
- Claridge, D. E.** (2006). Fine-scale distribution and habitat selection of beaked whales. *PhD thesis*, Aberdeen University, Aberdeen, UK.
- Clarke, M.** (2003). Production and control of sound by the small sperm whales, *Kogia breviceps* and *K. sima* and their implications for other Cetacea. *J. Mar. Biol. Assoc. UK.* **83**, 241–263. doi:10.1017/S0025315403007045h
- DeRuiter, S. L., Bahr, A., Blanchet, M.-A., Hansen, S. F., Kristensen, J. H., Madsen, P. T., Tyack, P. L. and Wahlberg, M.** (2009). Acoustic behaviour of echolocating porpoises during prey capture. *J. Exp. Biol.* **212**, 3100–3107. doi:10.1242/jeb.030825
- Duncan, A. J. and Maggi, A. L.** (2006). A consistent, user friendly interface for running a variety of underwater acoustic propagation codes. Proceedings of ACOUSTICS, pp. 471–477.
- Dunn, C. and Claridge, D.** (2014). Killer whale (*Orcinus orca*) occurrence and predation in the Bahamas. *J. Mar. Biol. Assoc. UK.* **94**, 1305–1309. doi:10.1017/S0025315413000908
- Dunphy-Daly, M. M., Heithaus, M. R. and Claridge, D. E.** (2008). Temporal variation in dwarf sperm whale (*Kogia sima*) habitat use and group size off Great Abaco Island, Bahamas. *Mar. Mamm. Sci.* **24**, 171–182. doi:10.1111/j.1748-7692.2007.00183.x
- Elwen, S. H., Gridley, T., Roux, J. P., Best, P. B. and Smale, M. J.** (2013). Records of kogiid whales in Namibia, including the first record of the dwarf sperm whale (*Kogia sima*). *Mar. Biodivers. Rec.* **6**, 1–9. doi:10.1017/S1755267212000942
- Fais, A., Johnson, M., Wilson, M., Aguilar de Soto, N. and Madsen, P. T.** (2016). Sperm whale predator-prey interactions involve chasing and buzzing, but no acoustic stunning. *Sci. Rep.* **6**, 28562. doi:10.1038/srep28562
- Finneran, J. J., Mulsow, J., Branstetter, B., Moore, P. and Houser, D. S.** (2016). Nearfield and farfield measurements of dolphin echolocation beam patterns: no evidence of focusing. *J. Acoust. Soc. Am.* **140**, 1346–1360. doi:10.1121/1.4961015
- Frasier, K. E., Wiggins, S. M., Harris, D., Marques, T. A., Thomas, L. and Hildebrand, J. A.** (2016). Delphinid echolocation click detection probability on near-seafloor sensors. *J. Acoust. Soc. Am.* **140**, 1918–1930. doi:10.1121/1.4962279
- Galatius, A., Olsen, M. T., Steeman, M. E., Racicot, R. A., Bradshaw, C. D., Kyhn, L. A. and Miller, L. A.** (2019). Raising your voice: evolution of narrow-band high-frequency signals in toothed whales (*Odontoceti*). *Biol. J. Linn. Soc.* **126**, 213–224. doi:10.1093/biolinnean/bly194
- Gillespie, D., Mellinger, D., Gordon, J., McLaren, D., Redmond, P., Mchugh, R., Trinder, P., Deng, X. Y. and Thode, A.** (2008). PAMGUARD: Semiautomated, open source software for real-time acoustic detection and localization of cetaceans. *J. Acoust. Soc. Am.* **30**, 54–62.
- Gkikopoulou, K. C.** (2018). Getting below the surface: Density estimation methods for deep diving animals using slow autonomous underwater vehicles. *PhD thesis*, University of St Andrews, St Andrews, UK.
- Goold, J. C. and Clarke, M. R.** (2000). Sound velocity in the head of the dwarf sperm whale, *Kogia sima*, with anatomical and functional discussion. *J. Mar. Biol. Assoc. UK.* **80**, 535–542. doi:10.1017/S002531540000223X
- Götz, T., Antunes, R. and Heinrich, S.** (2010). Echolocation clicks of free-ranging Chilean dolphins (*Cephalorhynchus eutropia*). *J. Acoust. Soc. Am.* **128**, 563–566. doi:10.1121/1.3353078
- Griffiths, E. T., Archer, F., Rankin, S., Keating, J. L., Keen, E., Barlow, J. and Moore, J. E.** (2020). Detection and classification of narrow-band high frequency echolocation clicks from drifting recorders. *J. Acoust. Soc. Am.* **147**, 3511–3522. doi:10.1121/1.0001229
- Hall, J. D. and Johnson, C. S.** (1972). Auditory thresholds of a killer whale *Orcinus orca* Linnaeus. *J. Acoust. Soc. Am.* **51**, 515–517. doi:10.1121/1.1912871
- Hildebrand, J. A., Frasier, K. E., Baumann-Pickering, S., Wiggins, S. M., Merkens, K. P., Garrison, L. P., Soldevilla, M. S. and McDonald, M. A.** (2019). Assessing seasonality and density from passive acoustic monitoring of signals presumed to be from pygmy and dwarf sperm whales in the Gulf of Mexico. *Front. Mar. Sci.* **6**, 66. doi:10.3389/fmars.2019.00066
- Hodge, L. E. W., Baumann-Pickering, S., Hildebrand, J. A., Bell, J. T., Cummings, E. W., Foley, H. J., McAlarney, R. J., McLellan, W. A., Pabst, D. A., Swaim, Z. T. et al.** (2018). Heard but not seen: Occurrence of *Kogia* spp. along the western North Atlantic shelf break. *Mar. Mamm. Sci.* **34**, 1141–1153. doi:10.1111/mms.12498
- Huggenberger, S., Rauschmann, M. A., Vogl, T. J., Oelschläger, H. H. A.** (2009). Functional Morphology of the Nasal Complex in the Harbor Porpoise (*Phocoena phocoena* L.). *Anatom. Rec.* **292**, 902–920. doi:10.1002/ar.20854
- Jensen, F. H., Rocco, A., Mansur, R. M., Smith, B. D., Janik, V. M. and Madsen, P. T.** (2013). Clicking in shallow rivers: short-range echolocation of Irrawaddy and Ganges river dolphins in a shallow, acoustically complex habitat. *PLoS ONE* **8**, e59284. doi:10.1371/journal.pone.0059284
- Jensen, F. H., Wahlberg, M., Beedholm, K., Johnson, M., Aguilar de Soto, N. and Madsen, P. T.** (2015). Single-click beam patterns suggest dynamic changes to the field of view of echolocating Atlantic spotted dolphins (*Stenella frontalis*) in the wild. *J. Exp. Biol.* **218**, 1314–1324. doi:10.1242/jeb.116285
- Jensen, F. H., Johnson, M., Ladegaard, M., Wisniewska, D. and Madsen, P. T.** (2018). Narrow acoustic field of view drives frequency scaling in toothed whale biosonar. *Curr. Biol.* **28**, 1–8. doi:10.1016/j.cub.2017.11.007
- Jensen, F. H., Keller, O. A., Tyack, P. L. and Visser, F.** (2020). Dynamic biosonar adjustment strategies in deep-diving Risso's dolphins driven partly by prey evasion. *J. Exp. Biol.* **223**, jeb216283. doi:10.1242/jeb.216283
- Johnson, M., Madsen, P. T., Zimmer, W. M., Aguilar de Soto, N. and Tyack, P. L.** (2004). Beaked whales echolocate on prey. *Proc. Roy. Soc. B.* **271**, S383–S386. doi:10.1098/rsbl.2004.0208
- Johnson, M., Madsen, P. T., Zimmer, W., Aguilar de Soto, N. and Tyack, P. T.** (2006). Foraging Blainville's beaked whales (*Mesoplodon densirostris*) produce distinct click types matched to different phases of echolocation. *J. Exp. Biol.* **209**, 5038–5050. doi:10.1242/jeb.02596
- Johnson, M., Hickmott, L., Aguilar de Soto, N. and Madsen, P. T.** (2008). Echolocation behaviour adapted to prey in foraging Blainville's beaked whale (*Mesoplodon densirostris*). *Proc. Roy. Soc. B.* **275**, 133–139. doi:10.1098/rspb.2007.1190
- Kadane, J. and Penner, R.** (1983). Range ambiguity and pulse interval jitter in the bottlenose dolphin. *J. Acoust. Soc. Am.* **74**, 1059–1061. doi:10.1121/1.389940
- Kastelein, R., Au, W., Rippe, H. and Schooneman, N.** (1999). Target detection by an echolocating harbor porpoise (*Phocoena phocoena*). *J. Acoust. Soc. Am.* **105**, 2493–2498. doi:10.1121/1.426951
- Kastelein, R. A., Bunskoek, P., Hagedoorn, M., Au, W. W. and de Haan, D.** (2002). Audiogram of a harbor porpoise (*Phocoena phocoena*) measured with narrow-band frequency-modulated signals. *J. Acoust. Soc. Am.* **112**, 334–344. doi:10.1121/1.1480835
- Kastelein, R. A., Janssen, M., Verboom, W. C. and de Haan, D.** (2005). Receiving beam patterns in the horizontal plane of a harbor porpoise (*Phocoena phocoena*). *J. Acoust. Soc. Am.* **118**, 1172–1179. doi:10.1121/1.1945565

- Ketten, D. R.** (2000). Cetacean ears. In *Hearing by Whales and Dolphins* (ed. W. W. Au and R. R. Fay), pp. 43–108. New York, USA: Springer.
- Koblitz, J. C., Wahlberg, M., Stilz, P., Madsen, P. T., Beedholm, K. and Schnitzler, H.-U.** (2012). Asymmetry and dynamics of a narrow sonar beam in an echolocating harbor porpoise. *J. Acoust. Soc. Am.* **131**, 2315–2324. doi:10.1121/1.3683254
- Koblitz, J. C., Stilz, P., Rasmussen, M. H. and Laidre, K. L.** (2016). Highly Directional Sonar Beam of Narwhals (*Monodon monoceros*) measured with a vertical 16 hydrophone array. *PLoS ONE* **11**, e0162069. doi:10.1371/journal.pone.0162069
- Kyhn, L. A., Tougaard, J., Jensen, F., Wahlberg, M., Stone, G., Yoshinaga, A., Beedholm, K. and Madsen, P. T.** (2009). Feeding at a high pitch: Source parameters of narrow band, high-frequency clicks from echolocating off-shore hourglass dolphins and coastal Hector's dolphins. *J. Acoust. Soc. Am.* **125**, 1783–1791. doi:10.1121/1.3075600
- Kyhn, L. A., Jensen, F. H., Beedholm, K., Tougaard, J., Hansen, M. and Madsen, P. T.** (2010). Echolocation in sympatric Peale's dolphins (*Lagenorhynchus australis*) and Commerson's dolphins (*Cephalorhynchus commersonii*) producing narrow-band high-frequency clicks. *J. Exp. Biol.* **213**, 1940–1949. doi:10.1242/jeb.042440
- Kyhn, L. A., Tougaard, J., Beedholm, K., Jensen, F. H., Ashe, E., Williams, R. and Madsen, P. T.** (2013). Clicking in a killer whale habitat: narrow-band, high-frequency biosonar clicks of harbour porpoise (*Phocoena phocoena*) and Dall's porpoise (*Phocoenoides dalli*). *PLoS ONE* **8**, e63763. doi:10.1371/journal.pone.0063763
- Ladegaard, M. and Madsen, P. T.** (2019). Context-dependent biosonar adjustments during active target approaches in echolocating harbour porpoises. *J. Exp. Biol.* **222**, jeb206169. doi:10.1242/jeb.206169
- Ladegaard, M., Jensen, F. H., de Freitas, M., da Silva, V. M. F. and Madsen, P. T.** (2015). Amazon river dolphins (*Inia geoffrensis*) use a high-frequency short-range biosonar. *J. Exp. Biol.* **218**, 3091–3101. doi:10.1242/jeb.120501
- Leoney, R. H., Carlslake, D. and Elwen, S. H.** (2011). Using static acoustic monitoring to describe echolocation behaviour of Heaviside's dolphins (*Cephalorhynchus heavisidii*) in Namibia. *Aquat. Mamm.* **37**, 151–160. doi:10.1578/AM.37.2.2011.151
- Macaulay, J.** (2020). Passive acoustic monitoring of harbour porpoise behaviour, distribution and density in tidal rapid habitats. PhD thesis, University of St Andrews, St Andrews, UK.
- Macaulay, J., Gordon, J., Gillespie, D., Malinka, C. and Northridge, S.** (2017). Passive acoustic methods for fine-scale tracking of harbour porpoises in tidal rapids. *J. Acoust. Soc. Am.* **141**, 1120–1132. doi:10.1121/1.4976077
- Macaulay, J., Malinka, C., Gillespie, D. and Madsen, P. T.** (2020). High resolution three-dimensional beam radiation pattern of harbour porpoise clicks with implications for passive acoustic monitoring. *J. Acoust. Soc. Am.* **147**, 4175–4188. doi:10.1121/10.0001376
- MacLeod, C. D., Hauser, N. and Peckham, H.** (2004). Diversity, relative density and structure of the cetacean community in summer months east of Great Abaco, Bahamas. *J. Mar. Biol. Assoc. UK* **84**, 469–474. doi:10.1017/S0025315404009476h
- Madsen, P. T. and Surlykke, A.** (2013). Functional Convergence in Bat and Toothed Whale. *Physiol.* **28**, 276–283. doi:10.1152/physiol.00008.2013
- Madsen, P. T. and Wahlberg, M.** (2007). Recording and quantification of ultrasonic echolocation clicks from free-ranging toothed whales. *Deep Sea Res. Part I Oceanogr. Res. Pap.* **54**, 1421–1444. doi:10.1016/j.dsr.2007.04.020
- Madsen, P. T., Payne, R., Kristiansen, N. U., Wahlberg, M., Kerr, I. and Møhl, B.** (2002). Sperm whale sound production studied with ultrasound time/depth-recording tags. *J. Exp. Biol.* **205**, 1899–1906.
- Madsen, P. T., Kerr, I. and Payne, R.** (2004). Echolocation clicks of two free-ranging, oceanic delphinids with different food preferences: false killer whales *Pseudorca crassidens* and Risso's dolphins *Grampus griseus*. *J. Exp. Biol.* **207**, 1811–1823. doi:10.1242/jeb.00966
- Madsen, P. T., Carder, D., Beedholm, K. and Ridgway, S.** (2005a). Porpoise clicks from a sperm whale nose—Convergent evolution of 130 kHz pulses in toothed whale sonars? *Bioacoust.* **15**, 195–206. doi:10.1080/09524622.2005.9753547
- Madsen, P. T., Johnson, M. P., Aguilar de Soto, N., Zimmer, W. M. X. and Tyack, P. L.** (2005b). Biosonar performance of foraging beaked whales (*Mesoplodon densirostris*). *J. Exp. Biol.* **208**, 181–194. doi:10.1242/jeb.01327
- Madsen, P. T., Wilson, M., Johnson, M., Hanlon, R. T., Bocconcelli, A., Aguilar de Soto, N. and Tyack, P. L.** (2007). Clicking for calamari: toothed whales can echolocate squid *Loligo pealeii*. *Aquat. Biol.* **1**, 141–150. doi:10.3354/ab00014
- Madsen, P. T., Aguilar de Soto, N., Arranz, P. and Johnson, M.** (2013). Echolocation in Blainville's beaked whales (*Mesoplodon densirostris*). *J. Comp. Phys. A* **199**, 451–469. doi:10.1007/s00359-013-0824-8
- Malinka, C. E., Atkins, J., Johnson, M. P., Tønnesen, P., Dunn, C. A., Claridge, D. E., Aguilar de Soto, N. and Madsen, P. T.** (2020). An autonomous hydrophone array to study the acoustic ecology of deep-water toothed whales. *Deep Sea Res. Part I Oceanogr. Res. Pap.* **158C**, 103233. doi:10.1016/j.dsr.2020.103233
- Marten, K.** (2000). Ultrasonic analysis of pygmy sperm whale (*Kogia breviceps*) and Hubbs' beaked whale (*Mesoplodon carlhubbsi*) clicks. *Aquat. Mamm.* **26**, 45–48.
- Martin, M. J., Gridley, T., Elwen, S. H. and Jensen, F. H.** (2018). Heaviside's dolphins (*Cephalorhynchus heavisidii*) relax acoustic crypsis to increase communication range. *Proc. Roy. Soc. B* **285**, 20181178. doi:10.1098/rspb.2018.1178
- McKenna, M. F., Cranford, T. W., Berta, A. and Pyenson, N. D.** (2012). Morphology of the odontocete melon and its implications for acoustic function. *Mar. Mamm. Sci.* **28**, 690–713. doi:10.1111/j.1748-7692.2011.00526.x
- Medwin, H.** (1975). Speed of sound in water: A simple equation for realistic parameters. *J. Acoust. Soc. Am.* **58**, 1318–1319. doi:10.1121/1.380790
- Merkens, K. P. and Oleson, E. M.** (2018). Comparison of High-frequency Echolocation Clicks (likely *Kogia*) in Two Simultaneously Collected Passive Acoustic Data Sets Sampled at 200 kHz and 320 kHz. NOAA Technical Memorandum NMFS-PIFSC-74.
- Merkens, K., Mann, D., Janik, V. M., Claridge, D., Hill, M. and Oleson, E.** (2018). Clicks of dwarf sperm whales (*Kogia sima*). *Mar. Mamm. Sci.* **34**, 963–978. doi:10.1111/mms.12488
- Morisaka, T. and Connor, R.** (2007). Predation by killer whales (*Orcinus orca*) and the evolution of whistle loss and narrow-band high frequency clicks in odontocetes. *J. Evol. Biol.* **20**, 1439–1458. doi:10.1111/j.1420-9101.2007.01336.x
- Møhl, B. and Andersen, S.** (1973). Echolocation: high-frequency component in the click of the Harbour Porpoise (*Phocoena ph. L.*). *J. Acoust. Soc. Am.* **54**, 1368–1372. doi:10.1121/1.1914435
- Moss, C. F. and Surlykke, A.** (2001). Auditory scene analysis by echolocation in bats. *J. Acoust. Soc. Am.* **110**, 2207–2226. doi:10.1121/1.1398051
- Møhl, B., Wahlberg, M., Madsen, P. T., Miller, L. A. and Surlykke, A.** (2000). Sperm whale clicks: Directionality and source level revisited. *J. Acoust. Soc. Am.* **107**, 638–648. doi:10.1121/1.428329
- Møhl, B., Wahlberg, M., Madsen, P. T., Heerfordt, A. and Lund, A.** (2003). The monopolised nature of sperm whale clicks. *J. Acoust. Soc. Am.* **114**, 1143–1154. doi:10.1121/1.1586258
- Moore, P., Hall, R., Friedl, W. and Nachtigall, P.** (1984). The critical interval in dolphin echolocation: What is it? *J. Acoust. Soc. Am.* **76**, 314–317. doi:10.1121/1.391016
- Pedersen, M. B., Tønnesen, P. H., Malinka, C. E., Ladegaard, M., Johnson, M., Aguilar de Soto, N. and Madsen, P. T.** (2021). Echolocation click parameters of short-finned pilot whales (*Globicephala macrorhynchus*) in the wild. *J. Acoust. Soc. Am.* **149** (in press). doi:10.1121/10.0003762
- Philips, J. D., Nachtigall, P. E., Au, W. W., Pawloski, J. L. and Roitblat, H. L.** (2003). Echolocation in the Risso's dolphin, *Grampus griseus*. *J. Acoust. Soc. Am.* **113**, 605–616. doi:10.1121/1.1527964
- Plön, S.** (2004). The status and natural history of pygmy (*Kogia breviceps*) and dwarf (*K. sima*) sperm whales off Southern Africa. PhD thesis, Rhodes University Grahamstown, South Africa.
- Reyes Reyes, M. V., Tossenberger, V. P., Iñiguez, M. A., Hildebrand, J. A. and Melcón, M. L.** (2016). Communication sounds of Commerson's dolphins (*Cephalorhynchus commersonii*) and contextual use of vocalizations. *Mar. Mamm. Sci.* **32**, 1219–1233. doi:10.1111/mms.12321
- Ridgway, S. and Carder, D.** (2001). Assessing hearing and sound production in cetaceans not available for behavioral audiograms: experiences with sperm, pygmy sperm, and gray whales. *Aquat. Mamm.* **27**, 267–276.
- Sato, M. and Benoit-Bird, K. J.** (2017). Spatial variability of deep scattering layers shapes the Bahamian mesopelagic ecosystem. *Mar. Ecol. Prog. Ser.* **580**, 69–82. doi:10.3354/meps12295
- Schnitzler, H.-U.** (1973). Control of Doppler shift compensation in the greater horseshoe bat, *Rhinolophus ferrumequinum*. *J. Comp. Phys.* **82**, 79–92. doi:10.1007/BF0014171
- Schnitzler, H.-U. and Kalko, E. K.** (2001). Echolocation by Insect-Eating Bats We define four distinct functional groups of bats and find differences in signal structure that correlate with the typical echolocation tasks faced by each group. *Biosci.* **51**, 557–569. doi:10.1641/0006-3568(2001)051[0557:EBIEB]2.0.CO;2
- Scott, M. D., Hohn, A. A., Westgate, A. J., Nicholar, J. R., Whitaker, B. R. and Campbell, W. B.** (2001). A note on the release and tracking of a rehabilitated pygmy sperm whale (*Kogia breviceps*). *J. Cetacean Res. Manag.* **3**, 87–94.
- Staudinger, M. D., McAlarney, R. J., McLellan, W. A. and Pabst, D. A.** (2014). Foraging ecology and niche overlap in pygmy (*Kogia breviceps*) and dwarf (*Kogia sima*) sperm whales from waters of the US mid-Atlantic coast. *Mar. Mamm. Sci.* **30**, 626–655. doi:10.1111/mms.12064
- Strother, G. and Mogus, M.** (1970). Acoustical beam patterns for bats: some theoretical considerations. *J. Acoust. Soc. Am.* **48**, 1430–1432. doi:10.1121/1.1912304
- Supin, A. Y. and Popov, V. V.** (1995). Temporal resolution in the dolphin's auditory system revealed by double-click evoked potential study. *J. Acoust. Soc. Am.* **97**, 2586–2593. doi:10.1121/1.411913
- Surlykke, A. and Moss, C. F.** (2000). Echolocation behavior of big brown bats, *Eptesicus fuscus*, in the field and the laboratory. *J. Acoust. Soc. Am.* **108**, 2419–2429. doi:10.1121/1.1315295
- Szymanski, M. D., Bain, D. E., Kiehl, K., Pennington, S., Wong, S. and Henry, K. R.** (1999). Killer whale (*Orcinus orca*) hearing: auditory brainstem response and behavioral audiograms. *J. Acoust. Soc. Am.* **106**, 1134–1141. doi:10.1121/1.427121
- Thomas, J., Moore, P., Nachtigall, P. and Gilmartin, W.** (1990). A new sound from a stranded pygmy sperm whale. *Aquat. Mamm.* **16**, 28–30.

- Thornton, S. W., Mclellan, W. A., Rommel, S. A., Dillaman, R. M., Nowacek, D. P., Koopman, H. N. and Pabst, D. A.** (2015). Morphology of the nasal apparatus in pygmy (*Kogia breviceps*) and dwarf (*K. sima*) sperm whales. *Anatom. Rec.* **298**, 1301-1326. doi:10.1002/ar.23168
- Tønnesen, P., Oliveira, C., Johnson, M. and Madsen, P. T.** (2020). The long-range echo scene of the sperm whale biosonar. *Biol. Lett.* **16**, 20200134. doi:10.1098/rsbl.2020.0134
- Urick, R. J.** (1983). *Principles of Underwater Sound*. Peninsula, Los Altos: McGraw-Hill.
- Vel'min, V. and Dubrovsky, N.** (1975). Auditory analysis of sound pulses in dolphins. *Dok. Akad. Nauk SSSR* **225**, 470-473.
- Verfuß, U. K., Miller, L. A., Pilz, P. K. and Schnitzler, H.-U.** (2009). Echolocation by two foraging harbour porpoises (*Phocoena phocoena*). *J. Exp. Biol.* **212**, 823-834. doi:10.1242/jeb.022137
- Villadsgaard, A., Wahlberg, M. and Tougaard, J.** (2007). Echolocation signals of wild harbour porpoises, *Phocoena phocoena*. *J. Exp. Biol.* **210**, 56-64. doi:10.1242/jeb.02618
- Wenz, G. M.** (1962). Acoustic ambient noise in the ocean: spectra and sources. *J. Acoust. Soc. Am.* **34**, 1936-1956. doi:10.1121/1.1909155
- Wiebe, P. H., Greene, C. H., Stanton, T. K. and Burczynski, J.** (1990). Sound scattering by live zooplankton and micronekton: empirical studies with a dual-beam acoustical system. *J. Acoust. Soc. Am.* **88**, 2346-2360. doi:10.1121/1.400077
- Willis, P. M. and Baird, R. W.** (1998). Status of the dwarf sperm whale, *Kogia simus*, with special reference to Canada. *Can. Field-Nat.* **112**, 114-125.
- Wisniewska, D. M., Johnson, M., Beedholm, K., Wahlberg, M. and Madsen, P. T.** (2012). Acoustic gaze adjustments during active target selection in echolocating porpoises. *J. Exp. Biol.* **215**, 4358-4373. doi:10.1242/jeb.074013
- Wisniewska, D. M., Johnson, M., Nachtigall, P. E. and Madsen, P. T.** (2014). Buzzing during biosonar-based interception of prey in the delphinids *Tursiops truncatus* and *Pseudorca crassidens*. *J. Exp. Biol.* **217**, 4279-4282. doi:10.1242/jeb.113415
- Wisniewska, D. M., Ratcliffe, J. M., Beedholm, K., Christensen, C. B., Johnson, M., Koblitz, J. C., Wahlberg, M. and Madsen, P. T.** (2015). Range-dependent flexibility in the acoustic field of view of echolocating porpoises (*Phocoena phocoena*). *eLife* **4**, e05651. doi:10.7554/eLife.05651
- Zimmer, W. M.** (2011). *Passive Acoustic Monitoring of Cetaceans*. Cambridge, UK: Cambridge University Press.
- Zimmer, W. M. X., Johnson, M., Madsen, P. T. and Tyack, P.** (2005). Echolocation clicks of free-ranging Cuvier's beaked whales (*Ziphius cavirostris*). *J. Acoust. Soc. Am.* **117**, 3919-3927. doi:10.1121/1.1910225